

An Analysis of the Corner Velocity Interpolation as the Approximation Space in a Mixed Finite Element Method

Master Thesis in Applied and Computational Mathematics

Morten Andreas Nome

Department of Mathematics
University of Bergen



June 6, 2008

Acknowledgements

I would like to thank especially Helge Dahle, Ivar Aavatsmark, Geir Terje Eigestad, Jan Martin Nordbotten, Håkon Hægland, Kristine Selvikvåg, Eirik Keilegavlen, and Jørn Hafver for invaluable help and cooperation during the work with this thesis. Special thanks to Tom Russell at the National Science Foundation for his hospitality and guidance during my visit to Washington D.C. November 2007. My sincerest thanks to *everyone* in the mathematics department, and to my mother.

Contents

Acknowledgements	i
1 Introduction	1
2 Background	3
2.1 Governing equations	3
2.2 Abstract formulation of the model problem	5
2.3 Construction of the mixed finite element method	8
2.4 Hexahedra through the trilinear mapping	11
2.4.1 The trilinear mapping	12
2.4.2 Three categories of hexahedra	15
2.5 Velocity interpolation and mixed methods	17
2.5.1 The space $H(\text{div})$	17
2.5.2 The coercivity condition	20
2.5.3 The inf-sup condition	21
2.5.4 Example: The space RT_0	21
3 Analysis of the corner velocity interpolation (CVI)	23
3.1 Construction of the interpolation and assembly of its basic properties	23
3.1.1 The CVI on cells with planar outer faces	23
3.1.2 The CVI on cells with curved outer faces	26
3.1.3 The divergence of the CVI	28
3.1.4 Local estimates for the CVI	30
3.2 The corner velocity interpolation with respect to mixed methods	31
3.2.1 The coercivity condition	32
3.2.2 The inf-sup condition	34
4 Summary	39
References	41

Chapter 1

Introduction

During the past decades, modeling flow in porous media has become an important branch of applied mathematics. The basic physical laws, for instance Darcy's law and the mass balance equation, are well established. But the physics governing flow in porous media can be made arbitrarily complicated, and work is still being done to incorporate more and more properties into the mathematical models.

Even in the simplest cases, the mathematical equations governing flow in porous media can rarely be solved analytically; some sort of numerical method has to be used to approximate most problems. There is a wide range of numerical methods that are being used for practical computations and theoretical studies. Some examples are finite element methods, control volume or finite difference methods, and multi-point flux methods. All numerical methods initially decompose the domain on which the equations are to be solved in a finite number of subdomains, called cells, and then assemble linear sets of equations for a finite number of values of the dependent variables being approximated.

In this thesis, we will focus on the so-called mixed finite element methods, and we will treat incompressible single-phase flow only. 'Single-phase' means that we will work with the mathematical models governing the flow of one fluid. This fluid will have only pressure and velocity as dependent variables. A good understanding of single-phase flow is indispensable for understanding multi-phase and multi-component flow; 'multi-phase'/'multi-component' means that there are several different immiscible fluids to account for, and these may exchange mass or components over fluid-fluid interfaces. This leads to very complex systems of nonlinear equations. However, it is in solving these systems the solution techniques for single-phase flow are of importance as building blocks.

The term 'mixed' in the mixed method refers to the fact that we are approximating the pressure and the velocity simultaneously. Many numerical methods first approximate the pressure, which is a harmonic function, and then uses the computed pressure to find the velocity. This approach usually leads to less accuracy in the velocity than in the pressure. The mixed finite element method compensates this by assembling only one linear system, where both the pressure and the velocity are unknowns.

Finite element methods are dependent on the so-called shape functions. A shape function is an interpolation of some dependent variable on a cell; for example, if the net fluxes across the different parts of the boundary of a cell are known, then this interpolation specifies the velocity function on the interior of that cell. While most numerical methods assemble their linear systems without regard to what the dependent variables look like aside from a finite number of computed values, a finite element method uses the shape functions both to construct the linear system for these values, and to provide a *function* which interpolates them.

For mixed finite element methods, there are two theoretical conditions which, when satisfied, imply convergence of the method. These conditions are called the inf-sup and coercivity conditions. Different mixed finite element methods are obtained by choosing different approximation spaces for the dependent variables of pressure and velocity, and whether they converge or not

depends on whether these two conditions are satisfied for the specific combination of pressure and approximation spaces. The approximation spaces are determined by the shape functions for the pressure and the velocity, so the question of convergence is really a question of whether the shape functions for the velocity and for the pressure together satisfy these conditions.

We now address the main problem of this thesis. In 2007, the corner velocity interpolation, abbreviated CVI, was introduced in a paper by H. Hægland et al. [9]. The CVI is a velocity interpolation scheme for general quadrilaterals in 2D and general hexahedra in 3D. This scheme was constructed for use in streamline simulation, an important branch of reservoir simulation. As mentioned above, most numerical methods do not provide a function which approximates the exact problem; only a finite set of function values, such as net fluxes of the velocity across a number of faces in the domain. When computing streamlines, one has to solve the ordinary differential equations

$$\frac{dy}{ds}(s, t) = v(y(s, t), t) \quad (1.1)$$

where $y \in \mathbb{R}^3$ is the streamline, $s \in \mathbb{R}$ is the streamline parameter, typically arc length, and v is some given velocity field. It is evident from (1.1) that for streamline simulation it is necessary to have a *function* v , not just a set of values indicating the general flow picture, and if the flow picture is computed by a method not specifying this function, then one has to interpolate the values of the approximation afterwards.

In [9] it is shown how many of the low-order velocity interpolation schemes commonly used for streamline tracing and mixed finite element methods do not preserve uniform flow. This is somewhat unsatisfactory. The issue is also treated in [10], in which an alternative shape function was proposed, which preserves uniform flow on certain hexahedral elements in 3D, but not on general elements.

The CVI was invented with the purpose of preserving uniform flow on general hexahedral elements. It was invented for streamline tracing, but a natural question to ask is: could the CVI be used in a mixed finite element method? Since the CVI is a velocity interpolation on general hexahedra, this determines a shape function for the velocity, which in turn determines an approximation space for the velocity on hexahedral grids. Together with a properly chosen pressure approximation space, there is hope that the mixed finite element method could benefit from the CVI's ability to reproduce uniform flow on general hexahedra.

However, it was shown in [12], that reproduction of uniform flow on hexahedra with curved faces is in conflict with the necessary regularity conditions on the velocity approximation space in mixed finite element methods. Implementing and testing the mixed finite element method on irregular grids is a complex task, and since there was reason to suspect non-convergence at least on grids with curved faces, we have chosen instead to investigate whether the corner velocity interpolation satisfies the coercivity and inf-sup conditions in combination with the space of constant pressures.

This thesis is organized as follows. Chapter 2 introduces the model problem, constructs the mixed finite element method for this problem, explains the necessary basics for working with velocity interpolations, and finally explains the inf-sup and coercivity conditions. Chapter 3 introduces the CVI and shows first that it reduces to a well-known approximation space for the velocity on parallelepiped grids, and then that the inf-sup and coercivity conditions do not hold for this space together with constant pressures on general grids. The results are summarized in Chapter 4.

Chapter 2

Background

This chapter explains the most basic equations governing flow in porous media, establishes the model problem, assembles its weak form, explains the construction of the mixed finite element method, introduces the necessary basics for working with velocity fields, and finally, explains briefly how the inf-sup and coercivity conditions relate to the velocity interpolation. A short treatment on whether the velocity interpolation is a member of the same space as the exact solution of the model problem is also included.

2.1 Governing equations

Introductions to the modeling of flow in porous media can be found in many textbooks, eg. [1], [3], [4], [5], and [13], and will only be treated briefly here.

The first of the equations governing one-phase flow in porous media flow, is

$$\frac{\partial \phi \rho}{\partial t} + \operatorname{div}(\rho v) = g, \quad (2.1)$$

usually called the mass balance equation, the conservation equation, or the continuity equation. Here ϕ is the porosity, ρ density, v velocity, and g is a source term. All variables are functions of space and time. The mass balance equation is derived from the assumption that what flows into a domain and what is created inside it should equal the net accumulation of mass in the domain. The porosity ϕ is the ratio between pore volume and total volume. It is treated as a piecewise continuous function with values between 0 and 1.

In a porous medium, due to the large friction between pore walls and fluid, the relation between fluid flow and pressure is governed by Darcy's law

$$v = -\frac{K}{\mu} Dp, \quad (2.2)$$

which says that the velocity v is proportional to the applied force. Here K is the permeability, μ viscosity, and p is the fluid pressure.

The permeability K is a square symmetric matrix measuring the medium's ability to transmit fluids. For a homogeneous medium, K is a matrix with constant entries k_{ij} , giving components of Darcy's law (2.2)

$$v_i = -\sum_{j=1}^3 \frac{k_{ij}}{\mu} \frac{\partial p}{\partial x_j}. \quad (2.3)$$

Symmetric matrices can always be diagonalized, so there is a coordinate system in which K is diagonal, simplifying Darcy's law to

$$v_i = -\frac{k_i}{\mu} \frac{\partial p}{\partial x_i}, \quad (2.4)$$

If the three entries of the diagonal matrix K are different, the medium is called anisotropic. This means that the permeability is dependent on the direction, ie. that every component of Darcy's law has its own permeability factor k_i . Usually the medium is also heterogeneous, which means that the entries of the permeability matrix are functions of space and time, giving $k_{ij} = k_{ij}(x, t)$ for all i, j . In this case the permeability cannot be expected to be continuous, as it models geological formations, with cracks, sudden changes in the porosity, and sharp interfaces between different rock types.

The source g is usually given as either a point source, or as a function of time and space. The physical interpretation of the latter case is that at every point there is or is not an injection or production of fluid given as volume per second and cube meter. In the former, the source is given as a Dirac delta function, giving a finite injection or production of mass per time unit when the production or injection point is inside some domain of integration.

We will conclude this section with setting up a well-posed mathematical formulation of a one-phase flow problem. Well-posed means (see [8], p. 7) that the problem

1. has a solution
2. the solution is unique and
3. the solution depends continuously on the boundary conditions.

The general question is, given a domain $\Omega \in \mathbb{R}^3$ with a polygonal boundary $\partial\Omega$, and boundary conditions $p = p_0$ on Γ_1 and $v \cdot n = v_0$ on Γ_2 , where $\Gamma_1 \cup \Gamma_2 = \partial\Omega$, what will the flow picture look like? To answer this question, we have to specify boundary conditions and some of the above parameters, and to keep things simple, these specifications will be:

- One-phase flow (p and v are the only dependent variables)
- Rigid rock (ϕ independent of time)
- Fluid incompressibility with the same density everywhere (ρ independent of time and space)
- Steady-state flow (general time-independence of p and v)
- Given, symmetric, positive definite permeability matrix
- $\mu = 1$
- $p = 0$ on $\Gamma_1 = \partial\Omega$

Equations (2.1) and (2.2) become, under these assumptions,

$$-Dp = K^{-1}v, \quad (2.5)$$

$$\operatorname{div}(v) = g. \quad (2.6)$$

It is possible to show that this problem is well-posed under certain regularity conditions on the source g . See [7].

Remark 2.1.1 *Note that we could also have inserted (2.2) into (2.6), to obtain*

$$-\operatorname{div}(K Dp) = g, \quad (2.7)$$

which is Laplace's equation.

Remark 2.1.2 *In the case of nonhomogeneous boundary values $p = p_0$ on $\partial\Omega$, it is possible to reduce to the homogeneous case. The result is that the boundary values are taken care of by the source g instead, and this is simpler to work with. The reduction to the homogeneous case is explained in [8], p. 297.*

2.2 Abstract formulation of the model problem

This chapter introduces the weak, or variational, formulation for the problem (2.6) and (2.5). We need this for two reasons. The first is that we have to allow for discontinuities in the permeability matrix K and the source g , so a regular differential equation is not the appropriate physical model for the flow. The second reason is that the weak formulation is the basis for constructing finite element methods.

Hilbert spaces and notation

Let V be a real linear space, that is, a space of real-valued functions for which $f, g \in V$ and $a, b \in \mathbb{R}$ implies $af + bg \in V$.

A norm on V is a mapping $\|\cdot\| : V \rightarrow \mathbb{R}^+$ which satisfies for all $f, g \in V, a \in \mathbb{R}$

- (i) $\|f + g\| \leq \|f\| + \|g\|$
- (ii) $\|ag\| = |a|\|g\|$
- (iii) $(f, f) = 0 \Leftrightarrow f = 0$

An inner product is a symmetric bilinear mapping $(\cdot, \cdot) : V \times V \rightarrow \mathbb{R}$ which satisfies

- (i) $(f, f) \geq 0 \quad \forall f \in V$
- (ii) $(f, f) = 0 \Leftrightarrow v = 0$

It is easy to show that

$$\|\cdot\| = \sqrt{(f, f)}, \quad f \in V \quad (2.8)$$

defines a norm on V . A space V is *complete* if it has an inner product and every Cauchy sequence in V converges in the norm (2.8) to a limit in V . Complete spaces are called Hilbert spaces, and Hilbert spaces will be denoted H throughout this section. Two important Hilbert spaces are:

$L^2(\Omega)$, the space of square integrable functions on Ω : $\{f : \int_{\Omega} f^2 dx < \infty\}$. L^2 has the inner product $(f, g) = \int_{\Omega} fg dx$.

$H(\text{div}, \Omega)$, the space of vector functions $\{f : f \in L^2(\Omega)^3; \text{div}(f) \in L^2(\Omega)\}$. $H(\text{div}, \Omega)$ has the inner product $(f, g) = \int_{\Omega} \sum_i f_i g_i + \text{div}(f) \text{div}(g) dx$.

These are the only two Hilbert spaces we will need. For the sake of brevity, $L^2(\Omega)$ will be denoted Q . Arbitrary elements from Q will be denoted q , specific pressure solutions of problems such as (2.5) will be denoted p . Similarly, $H(\text{div}, \Omega)$ will be denoted W . Arbitrary elements from W will be denoted w , specific velocity solutions of problems such as (2.6) and (2.5) will be denoted v . Both spaces have norms $\|\cdot\| = \sqrt{(\cdot, \cdot)}$. When we write $\|\cdot\|$, we shall always mean $\|\cdot\|_W$ for $w \in W$, and $\|\cdot\|_Q$ for $q \in Q$. The derivatives in $\text{div}(f)$ are to be understood in a weak sense; see [8], p.242, for a definition of this.

A *functional* is a mapping $F : H \rightarrow \mathbb{R}$, which is said to be bounded if

$$\sup \{F(g); g \in H, \|g\| \leq 1\} < \infty, \quad (2.9)$$

The dual space of H , denoted H' , is the space of all bounded linear functionals on H . A famous theorem due to Riesz and Frechet, states that a Hilbert space is its own dual:

Theorem 2.2.1 (Riesz-Frechet) *For any $F \in H'$, there is a unique $h \in H$ such that*

$$F(g) = (g, h) \quad \forall g \in H. \quad (2.10)$$

For the proof, see [16], p. 63.

Investigating partial differential equations and approximation of them, often reduces to investigating bilinear forms, of which the inner product is a special case. The Riesz-Frechet theorem has an important generalization known as the Lax-Milgram theorem.

Let $a(\cdot, \cdot) : G \times G \rightarrow \mathbb{R}$ be a bilinear form on the closed subspace G of H . $a(\cdot, \cdot)$ is said to be continuous on G if there is a constant C such that

$$|a(f, g)| \leq C \|f\| \|g\| \quad f, g \in G, \quad (2.11)$$

and coercive on G if there is a constant α such that

$$\alpha \|f\|^2 \leq a(f, f) \quad f \in G. \quad (2.12)$$

Theorem 2.2.2 (Lax-Milgram) *Given a continuous and coercive bilinear form $a(\cdot, \cdot)$, there is for any $F \in G'$ a unique $h \in G$ such that*

$$F(g) = a(g, h) \quad \forall g \in G. \quad (2.13)$$

The proof can be found in [8], p.298. Note carefully that we have assumed nothing on the symmetry of $a(\cdot, \cdot)$.

The weak formulation and its well-posedness

In this section we will construct the weak, or variational formulation of (2.6) and (2.5). First multiply (2.5) with $w \in W$, (2.6) with $q \in Q$, and then integrate over Ω to get

$$\int_{\Omega} K^{-1}v \cdot w \, dx + \int_{\Omega} p \operatorname{div}(w) \, dx = 0, \quad (2.14)$$

$$\int_{\Omega} q \operatorname{div}(v) \, dx = \int_{\Omega} gq \, dx, \quad (2.15)$$

Note the integration by parts in the second term of the first equation. The boundary terms drop out because of the zero boundary conditions.

Note that a solution of (2.6) and (2.5) solves the weak problem, but the converse holds only for sufficiently smooth p and v . Weak formulations are usually constructed from a differential equation in such a way that the solution of the differential equation solves the weak formulation, but not necessarily vice versa. In this regard, the weak formulation represents an expansion of the solution set of the problem, and hence if the original problem had a solution, the solution of the corresponding weak problem cannot be assumed to be unique. See [8], section 3.4.

If we define

$$G(q) = \int_{\Omega} gq \, dx, \quad (2.16)$$

$$a(v, w) = \int_{\Omega} K^{-1}v \cdot w \, dx, \quad (2.17)$$

$$b(q, w) = \int_{\Omega} q \operatorname{div}(w) \, dx, \quad (2.18)$$

then the weak formulation is: find $v \in W$, $p \in Q$, solving

$$a(v, w) + b(p, w) = 0 \quad \forall w \in W, \quad (2.19)$$

$$b(q, v) = G(q) \quad \forall q \in Q. \quad (2.20)$$

It can be shown that (2.19) and (2.20) has a unique solution if the following holds:

(i) the forms $a(\cdot, \cdot) : W \times W \rightarrow \mathbb{R}$ and $b(\cdot, \cdot) : Q \times W \rightarrow \mathbb{R}$ are both continuous, that is, there exists constants C_a and C_b such that

$$\begin{aligned} a(v, w) &\leq C_a \|v\| \|w\| \quad \forall v, w \in W \\ b(q, w) &\leq C_b \|q\| \|w\| \quad \forall q \in Q, w \in W \end{aligned} \quad (2.21)$$

(ii) $a(\cdot, \cdot)$ is coercive on the space $Z = \{w \in W : \operatorname{div}(w) = 0\}$, that is, there exists a constant α such that

$$\alpha \|w\|^2 \leq a(w, w) \quad \forall w \in Z, \quad (2.22)$$

and

(iii) There exists a constant β such that for every $q \in Q$, there is a $w \in W$ satisfying

$$\beta \|q\| \|w\| \leq b(q, w). \quad (2.23)$$

It is possible to show that the conditions (i)-(iii) are satisfied for our definitions of $a(\cdot, \cdot)$ and $b(\cdot, \cdot)$. Note that the space Z can be written as the kernel of a bounded linear operator:

$$Z = \{w \in W : b(q, w) = 0 \quad \forall q \in Q\}, \quad (2.24)$$

which implies that it is a Hilbert space. See [7] for details.

To see how (i)-(iii) guarantees that a unique solution of (2.19) and (2.20) exists, first consider the following subproblem: find $v \in W$ solving

$$a(v, w) = 0 \quad \forall w \in Z, \quad (2.25)$$

$$b(v, q) = G(q) \quad \forall q \in Q. \quad (2.26)$$

This problem is well-posed, and this can be seen as follows. Assume that we have a particular solution v_1 of (2.26). This is really just solving $\operatorname{div}(v_1) = g$, which is an underdetermined problem (with many solutions) that can always be solved as long as $g \in L^2(\Omega)$ and $\partial\Omega$ is smooth or polygonal, see [6], p. 282. Then a general solution of (2.26) can be written $v = v_0 + v_1$, where v_0 is an arbitrary element of Z . Now $F_{v_1}(w) = a(v_1, w)$ is for every v_1 a bounded linear functional on Z , and we have (ii), so the Lax-Milgram theorem implies that the problem to find $v_0 \in Z$ such that

$$a(v_0, w) = F_{v_1}(w) \quad \forall w \in Z \quad (2.27)$$

has a unique solution for every v_1 . But $v = v_0 + v_1$ solving (2.25) and (2.26) does not depend on the choice of v_1 : if we have two solutions v and u of (2.25) and (2.26), then $v - u$ lies in Z , solves

$$a(v - u, w) = 0 \quad \forall w \in Z, \quad (2.28)$$

and the coercivity of $a(\cdot, \cdot)$ on Z implies $v - u = 0$.

Since any solution of (2.19) and (2.20) obviously solves (2.25) and (2.26), and this problem has a unique solution, we see that the velocity part of the solution of (2.19) and (2.20) is unique if it exists. With v well defined by (2.25) and (2.26), we may thus proceed to find p by considering: given v defined by (2.25) and (2.26), find $p \in Q$ such that

$$b(p, w) = -a(v, w) \quad \forall w \in W. \quad (2.29)$$

This problem has a unique solution if (iii) holds. This is a weaker kind of coercivity than the coercivity for $a(\cdot, \cdot)$, but has the necessary implications needed to prove well-posedness of (2.29). The proof of this is somewhat more involved than the proof of well-posedness of (2.27), and can be found in [6] p. 303.

2.3 Construction of the mixed finite element method

This section gives a short introduction to general finite elements, and then constructs the mixed finite element method for the problem (2.19) and (2.20).

Finite element methods in general

A finite element method is constructed according to the following recipe. First reformulate the original differential equation as in the preceding section. A standard problem to end up with is: find $f \in G$ satisfying

$$a(f, g) = F(g) \quad \forall g \in G, \quad (2.30)$$

where $F \in G'$ is the integral of the right hand side of the differential equation, $a(\cdot, \cdot)$ is some bilinear form relating to the equation's left hand side, and G is a closed subspace of a Hilbert space H .

Example 2.3.1 *If we multiply eq. (2.7) with a function w in a sufficiently smooth space G , integrate over Ω , and then integrate by parts, we get*

$$\int_{\Omega} f w \, dx = \int_{\Omega} (Dw)^T K(Dv) \, dx. \quad (2.31)$$

The problem is then: find v solving

$$a(w, v) = F(w) \quad \forall w \in G, \quad (2.32)$$

where

$$a(w, v) = \int_{\Omega} (Dw)^T K(Dv) \, dx, \quad F(w) = \int_{\Omega} f w \, dx. \quad (2.33)$$

See [1], p. 26.

Then decompose the domain on which the equation is to be solved, into a finite number of subdomains, such as hexahedrons or tetrahedrons (depicted below), and construct basis or shape functions for each subdomain. A shape function is a function on the interior of each cell Ω_i which depends on the spacial coordinates and a few parameters for each cell, called the degrees of freedom. A degree of freedom for a shape function is defined as the value of a functional, which is usually evaluation at a point in the cell for scalar fields, and the integral of the normal trace over an outer cell face for vector fields. The set of all degrees of freedom in the grid and a specific choice of shape functions define an approximation space which we denote G_h ; a specification of all degrees of freedom in the grid determines a member g_h of the approximation space. The subscript h refers to a typical length in the grid, such as the length of its shortest edge or the diameter of the largest ball inscribed in its smallest cell.

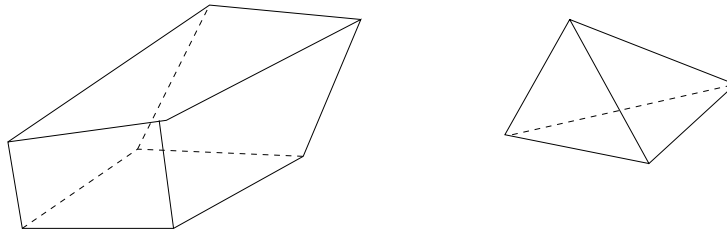


Figure 2.1: A hexahedron (left) and a tetrahedron (right).

The finite element method then determines a specific member f_h of the approximation space by solving

$$a(f_h, g_h) = F(g_h) \quad \forall g_h \in G_h, \quad (2.34)$$

which defines a linear system for the degrees of freedom of f_h . The following theorem quantifies the distance from the solution of (2.34) and (2.30):

Theorem 2.3.1 *Assume that*

- H is a Hilbert space,*
 - G is a closed subspace of H ,*
 - $a(\cdot, \cdot)$ is continuous and coercive on G ,*
 - $F \in G'$,*
 - $G_h \subseteq G$,*
 - f solves (2.30), and*
 - f_h solves (2.34).*
- Then the linear system 2.34 is nonsingular, and*

$$\|f - f_h\|_G \leq \frac{C}{\alpha} \min_{g \in G_h} \|f - g\|_G, \quad (2.35)$$

where C and α are the continuity and coercivity constants of a , respectively.

The proof of this theorem may be found in [6], pp. 63 and 64. The nonsingularity of (2.34) follows from the Lax-Milgram theorem. Note that the five first assumptions made here are the same as for the Lax-Milgram theorem.

In the next chapter, we will encounter a situation where the condition $G_h \not\subseteq G$ will have to be relaxed. This is called a variational crime, which refers to the fact that we are then approximating a function in a certain space G , by a function which is not necessarily in G . Without the assumption $G_h \subseteq G$, it is still possible to prove error estimates as long as $G_h \subseteq H$, but the bounds depend on $G_h \not\subseteq G$, and these may behave badly.

Theorem 2.3.2 *Assume that*

- H is a Hilbert space,*
 - G is a closed subspace of H ,*
 - $a(\cdot, \cdot)$ is continuous and coercive on $G \cup G_h$,*
 - $F \in G'$,*
 - $G_h \subseteq G$,*
 - f solves (2.30), and*
 - f_h solves (2.34).*
- Then*

$$\|f - f_h\|_H \leq \left(1 + \frac{C}{\alpha}\right) \min_{g \in G_h} \|f - g\|_H + \frac{1}{\alpha} \sup_{g \in G_h \setminus \{0\}} \frac{|a(f - f_h, g)|}{\|g\|_H}. \quad (2.36)$$

The proof may be found in ([6], p. 258).

The mixed finite element method

The mixed finite element method is constructed by taking finite-dimensional subspaces Q_h and W_h of the spaces Q and W in (2.19) and (2.20), and solving the following problem: find $p_h \in Q_h$ and $v_h \in W_h$, satisfying

$$a(v_h, w) + b(p_h, w) = 0 \quad \forall w \in W_h, \quad (2.37)$$

$$b(q, v_h) = F(q) \quad \forall q \in Q_h. \quad (2.38)$$

For Q_h , we will use the space of constant pressures. A member q_h of this space is characterized by a set of constants q_i ; each q_i is a degree of freedom specifying the constant pressure in the cell

Ω_i , and the number of degrees of freedom for q_h is thus equal to the number of cells in the grid. This space is so simple that it is not necessary with shape functions to describe it.

A typical degree of freedom for the velocity is the net flux across a face in the grid, and a shape function for the velocity is a function with unit flux across one face in the grid and no flux across the others. The number of degrees of freedom and of shape functions is then equal to the number of faces in the grid, and a member w_h of W_h is obtained by taking a linear combination of the fluxes and the corresponding shape functions.

As in the preceding section, (2.37) and (2.38) defines a linear system for the degrees of freedom of p_h and v_h . First we have to check that it is nonsingular.

Lemma 2.3.3 *The linear system (2.37) and (2.38) has a unique solution if there exists a constant β_h such that for every $q_h \in Q_h$, there is a $w_h \in W_h$ satisfying*

$$\beta_h \|q_h\| \|w_h\| \leq b(q_h, w_h). \quad (2.39)$$

The proof can be found in [14], p. 231. This lemma is necessary for convergence, but not sufficient.

Define

$$Z_h = \left\{ w_h \in W_h : \int_{\Omega} q_h \operatorname{div}(w_h) dy = 0 \quad \forall q_h \in Q_h \right\}. \quad (2.40)$$

It is possible to show that the solution (v_h, p_h) of (2.37) and (2.38) converges to the solution (v, p) of (2.14) and (2.15) as $h \rightarrow 0$ if there exists $\alpha > 0$ and $\beta > 0$, independent of the grid, such that

$$\alpha_h \|w_h\| \leq a(w_h, w_h) \quad \forall w \in Z_h, \quad (2.41)$$

and

$$\beta_h \|q_h\| \leq \sup_{w_h \in W_h} \frac{b(q_h, w_h)}{\|w_h\|} \quad \forall q_h \in Q_h, \quad (2.42)$$

where

$$Z_h = \{w_h \in W_h : b(q_h, w_h) = 0 \quad \forall q_h \in Q_h\}, \quad (2.43)$$

and

$$\alpha \leq \alpha_h, \quad \beta \leq \beta_h \quad \text{as } h \rightarrow 0. \quad (2.44)$$

The reason for the strict inequalities $\alpha > 0$ and $\beta > 0$ will become clear when we have assembled the error estimates. Note that both inequalities depend on W_h , Q_h , and, as we will see in the next chapter, on the choice of grid. When (2.41) holds with $\alpha > 0$ independent of the grid, the method is said to be coercive. Condition (2.42) is called the inf-sup condition. Eqs. (2.39) and (2.42) are obviously equivalent formulations of this inequality.

Remark 2.3.1 *A third equivalent formulation of the inf-sup condition, which gives rise to its name, is*

$$\beta_h \leq \inf_{q \in Q_h} \sup_{w_h \in W_h} \frac{b(q_h, w_h)}{\|w_h\| \|q_h\|}. \quad (2.45)$$

We now record some error estimates for the mixed finite element method.

Theorem 2.3.4 *If $W_h \subseteq W$, $Q_h \subseteq Q$, (2.41) holds for all $w \in Z_h \cup Z$, (v, p) is determined by (2.14) and (2.15), and (v_h, p_h) is determined by (2.37) and (2.38), then (2.36) gives*

$$\|v - v_h\| \leq \left(1 + \frac{C}{\alpha}\right) \inf_{w \in Z_h} \|v - w\| + \frac{C}{\alpha} \inf_{q \in Q_h} \|p - q\|. \quad (2.46)$$

If in addition, the inf-sup condition (2.42) holds, then

$$\|p - p_h\| \leq c \inf_{w \in Z_h} \|v - w\| + (1 + c) \inf_{q \in Q_h} \|p - q\|, \quad (2.47)$$

where $c = \frac{C}{\beta}(1 + \frac{C}{\alpha})$.

The proofs of (2.46) and (2.47) may be found in [6], pp. 305 and 313, respectively. Note that (2.46) depends on $1/\alpha$, and (2.47) depends on both $1/\alpha$ and $1/\beta$. This is why we need existence of α and β both strictly greater than zero as $h \rightarrow 0$.

2.4 Hexahedra through the trilinear mapping

Recall that the CVI is a velocity interpolation on hexahedral cells. This section introduces the trilinear mapping and shows how it is used to construct different hexahedra.

Notation

$x = (x_1, x_2, x_3) \in \mathbb{R}^3$ is a point in reference space. K is the unit cube in reference space: $K = \{x : 0 \leq x_i \leq 1, i = 1, 2, 3\}$, and ∂K is its boundary.

$y = (y_1, y_2, y_3) \in \mathbb{R}^3$ is a point in physical space.

Ω is a polygonal domain in physical space.

$y_i(x)$ is the trilinear transformation from reference space to physical space defined below.

Ω_i is a hexahedron in physical space, with vertices c_l , $l = 1, 2, \dots, 8$.

$w_i = (w_1, w_2, w_3) \in \mathbb{R}^3$ is the Darcy velocity on Ω_i . A uniform flow field is a flow field where the Darcy velocity is independent of the space coordinates (ie. constant), and will usually be denoted w_0 .

$e_{kl} = c_l - c_k$ is the edge from c_k to c_l of Ω_i . t_{kl} is the tangent vector along e_{kl} .

Γ_{ij} is one of the six outer faces of $\partial\Omega_i$, with area A_{ij} .

f_{ij} is the net outflux across the face Γ_{ij} of Ω_i .

n_{ij} is the outwards pointing unit normal vector of Γ_{ij} . Occasionally we will need the non-normalized normal vector \hat{n}_{ij} , to be defined below.

W is short-hand for the space $H(\text{div}, \Omega)$. W_h is an approximation space for the velocity, for which we may or may not have $W_h \subseteq W$. From now on, we drop the subscript h for members w of W_h , as we will need this subscript for other means in chapter 3.

ψ_{ij} is the velocity shape function on Ω_i with flux one through the face Γ_{ij} , and zero flux through the other faces.

Velocity means here flux density, measured in meters per second, as opposed to the flux, which is the total volume passing through a specific surface, measured in cube meters per second. Aside from a few exceptions, i will be used to keep track of cells, k keeps track of coordinate directions, j keeps track of faces, and l keeps track of vertices. With $(\cdot)_k$, we always mean the k 'th component. Note that K is used both to denote the reference cube and the permeability matrix, but there is of course never any danger of mixing up these two. Occasionally we will use non-indexed Γ , and in these cases we write A_Γ , n_Γ , and f_Γ . We have not tagged the edges, as it is always obvious from the context which cells they belong to.

2.4.1 The trilinear mapping

This subsection defines the trilinear mapping, assembles some of its properties, and explains the parametrized velocity field.

There are essentially two ways of representing a velocity field on a cell Ω_i : simply as a function of variables in physical space, or as a parametrization, that is, depending on variables in some reference space. The former is a map $w_i : \Omega_i \rightarrow \mathbb{R}^3$, where each of the components $w_i(y)$ is a function of the physical coordinates.

To describe the parametrized velocity field, we need to introduce the trilinear mapping $y_i(x)$. If $x = (x_1, x_2, x_3)$ is a point in reference space, then the corresponding point $y_i(x)$ in physical space is

$$\begin{aligned}
 y_i(x) = & c_1(1-x_1)(1-x_2)(1-x_3) + c_2x_1(1-x_2)(1-x_3) + c_3x_1x_2(1-x_3) + \\
 & c_4(1-x_1)x_2(1-x_3) + c_5(1-x_1)(1-x_2)x_3 + c_6x_1(1-x_2)x_3 + \\
 & c_7x_1x_2x_3 + c_8(1-x_1)x_2x_3 = \sum_{l=1}^8 c_l \phi_l(x), \quad (2.48)
 \end{aligned}$$

where c_l are the vertices (in physical space) of the hexahedron Ω_i . We then define Ω_i as the image of the reference cube K under the trilinear mapping:

$$\Omega_i = \{y_i(x); x \in K\}, \quad (2.49)$$

and

$$\partial\Omega_i = \{y_i(x); x \in \partial K\}. \quad (2.50)$$

Note that the vertices of K are mapped to the vertices of Ω_i . We have chosen the following correspondence between these two sets of vertices (see also fig. 2.2 below):

K	Ω_i
(0, 0, 0)	c_1
(1, 0, 0)	c_2
(1, 1, 0)	c_3
(0, 1, 0)	c_4
(0, 0, 1)	c_5
(1, 0, 1)	c_6
(1, 1, 1)	c_7
(0, 1, 1)	c_8

A parametrized velocity field on Ω_i can now be defined as a mapping $(y_i(x), w_i(x)) : K \rightarrow \mathbb{R}^6$, where $y_i(x)$ is a point in physical space, and w_i is the corresponding Darcy velocity at y_i .

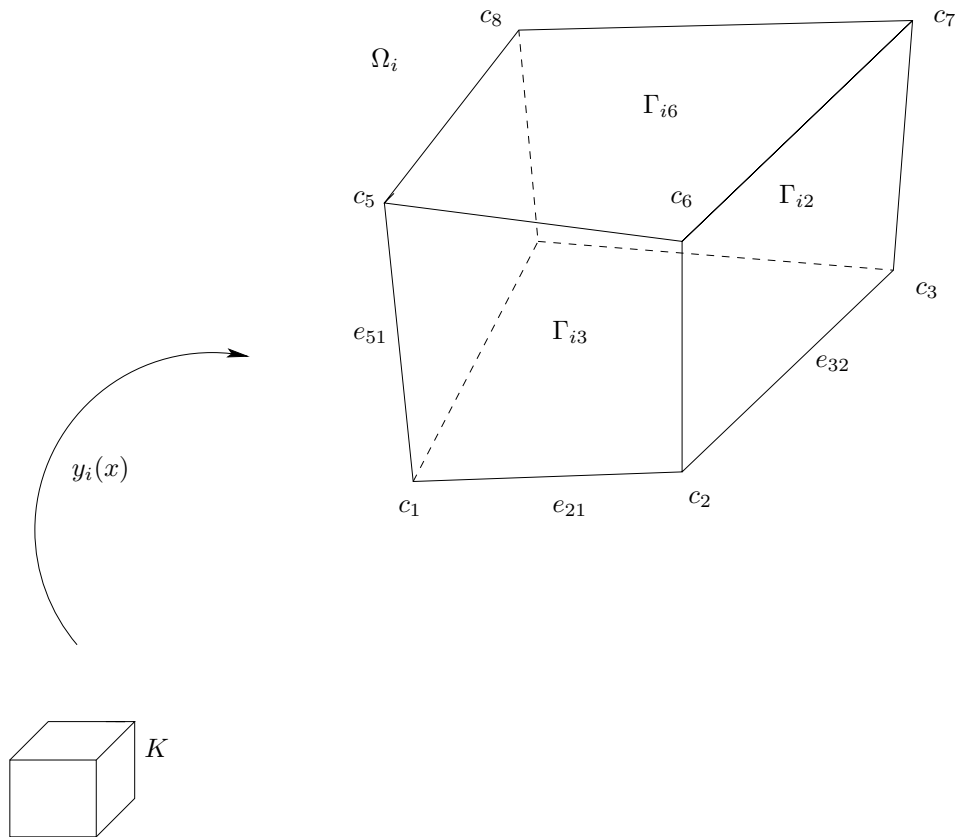


Figure 2.2: The trilinear transformation $y_i(x)$ maps the unit cube K onto a hexahedron defined by the vertices c_l . See below for the numbering of the faces Γ_{ij} .

We need to assemble a few properties of the trilinear mapping $y_i(x)$. The reason for this is that Ω_i is defined by this mapping and the eight vertices, so the shape of Ω_i is not at all obvious except for the positions of its eight vertices, and any geometric argument has to be based on properties of $y_i(x)$. Note that whether the mapping $y_i(x)$ maps the unit cube onto a proper hexahedron is dependent both on the numbering of the vertices c_l , and their coordinates. This is actually an interesting topic in its own right, and a very important one, as it is necessary to have robust grid generation methods that do not produce degenerate cells, but details are omitted here. See [15].

Denote by Γ_{x_i} an inner face defined by a fixed value of x_i . The covariant vectors of $y_i(x)$ are $\frac{\partial y_i}{\partial x_1}$, $\frac{\partial y_i}{\partial x_2}$ and $\frac{\partial y_i}{\partial x_3}$, and these can be used to define the unit normal vector of such a surface. For instance, when we fix x_1 ,

$$n = \frac{\frac{\partial y_i}{\partial x_2} \times \frac{\partial y_i}{\partial x_3}}{\left\| \frac{\partial y_i}{\partial x_2} \times \frac{\partial y_i}{\partial x_3} \right\|}, \quad (2.51)$$

and

$$\hat{n} = \frac{\partial y_i}{\partial x_2} \times \frac{\partial y_i}{\partial x_3}. \quad (2.52)$$

Observe that (2.51) is *the* unit normal vector of Γ_{x_1} since it obviously is normal to both of the vectors defining the osculating plane of Γ_{x_1} ($\frac{\partial y_i}{\partial x_2}$ and $\frac{\partial y_i}{\partial x_3}$), and has length one.

In the next section we will need an explicit formula for the normal vector, and this can be done as follows. We have

$$\begin{aligned} \frac{\partial y_i}{\partial x_2} = & -c_1(1-x_1)(1-x_3) - c_2x_1(1-x_3) + c_3x_1(1-x_3) + \\ & c_4(1-x_1)(1-x_3) - c_5(1-x_1)x_3 - c_6x_1x_3 + c_7x_1x_3 + c_8(1-x_1)x_3 = \\ & e_{41}(1-x_1)(1-x_3) + e_{32}x_1(1-x_3) + e_{76}x_1x_3 + e_{85}(1-x_1)x_3, \end{aligned} \quad (2.53)$$

and

$$\begin{aligned} \frac{\partial y_i}{\partial x_3} = & -(c_1(1-x_1)(1-x_2) + c_2x_1(1-x_2) + c_3x_1x_2 + c_4(1-x_1)x_2) \\ & + c_5(1-x_1)(1-x_2) + c_6x_1(1-x_2) + c_7x_1x_2 + c_8(1-x_1)x_2 = \end{aligned} \quad (2.54)$$

$$e_{51}(1-x_1)(1-x_2) + e_{62}x_1(1-x_2) + e_{73}x_1x_2 + e_{84}(1-x_1)x_2, \quad (2.55)$$

which, when for example $x_1 = 1$, simplify to

$$\frac{\partial y_i}{\partial x_2} = e_{32}(1-x_3) + e_{76}x_3, \quad (2.56)$$

and

$$\frac{\partial y_i}{\partial x_3} = e_{62}(1-x_2) + e_{73}x_2. \quad (2.57)$$

This gives

$$\begin{aligned} \hat{n} = & \quad (2.58) \\ & \left(\begin{array}{l} (e_{32}^2(1-x_3) + e_{76}^2x_3)(e_{62}^3(1-x_2) + e_{73}^3x_2) - (e_{32}^3(1-x_3) + e_{76}^3x_3)(e_{62}^2(1-x_2) + e_{73}^2x_2) \\ (e_{32}^3(1-x_3) + e_{76}^3x_3)(e_{62}^1(1-x_2) + e_{73}^1x_2) - (e_{32}^1(1-x_3) + e_{76}^1x_3)(e_{62}^3(1-x_2) + e_{73}^3x_2) \\ (e_{32}^1(1-x_3) + e_{76}^1x_3)(e_{62}^2(1-x_2) + e_{73}^2x_2) - (e_{32}^2(1-x_3) + e_{76}^2x_3)(e_{62}^1(1-x_2) + e_{73}^1x_2) \end{array} \right), \end{aligned}$$

where the superscripts are used to denote components. The computation for any other normal vector is analogous.

The volumetric jacobian of the trilinear mapping is

$$J = \det \frac{\partial y_i}{\partial x} = \frac{\partial y_i}{\partial x_1} \cdot \frac{\partial y_i}{\partial x_2} \times \frac{\partial y_i}{\partial x_3}. \quad (2.59)$$

It is natural to assume that this quantity is bounded away from zero, and this is true as long as the three covariant vectors are nowhere coplanar. An explicit bound from below, which will be useful below, can be deduced as follows. We have

$$\frac{\partial y_i}{\partial x_1} \cdot \frac{\partial y_i}{\partial x_2} \times \frac{\partial y_i}{\partial x_3} = \left| \frac{\partial y_i}{\partial x_1} \right| \left| \frac{\partial y_i}{\partial x_2} \right| \left| \frac{\partial y_i}{\partial x_3} \right| \sin \theta_1 \cos \theta_2, \quad (2.60)$$

where θ_1 is the angle between $\frac{\partial y_i}{\partial x_2}$, and $\frac{\partial y_i}{\partial x_3}$, and θ_2 is the angle between $\frac{\partial y_i}{\partial x_1}$ and $\frac{\partial y_i}{\partial x_2} \times \frac{\partial y_i}{\partial x_3}$. Now $\left| \frac{\partial y_i}{\partial x_1} \right|$, $\left| \frac{\partial y_i}{\partial x_2} \right|$, and $\left| \frac{\partial y_i}{\partial x_3} \right|$ take their minimum values at the edges of the reference cube corresponding to the shortest edges of the cell in physical space in the x_1 -, x_2 - and x_3 -directions, respectively:

$$\left| \frac{\partial y_i}{\partial x_1} \right| \geq \min_{k=21,34,65,78} |e_k| > 0; \quad (2.61)$$

the expressions for $\frac{\partial y_i}{\partial x_2}$, and $\frac{\partial y_i}{\partial x_3}$ are similar. The assumption of non-coplanarity is made explicit through

$$0 < \alpha_i \leq \theta_1, \quad \theta_2 \leq \beta_i < \pi/2 \quad \forall x \in K, \quad (2.62)$$

and we thus conclude

$$J = \frac{\partial y_i}{\partial x_1} \cdot \frac{\partial y_i}{\partial x_2} \times \frac{\partial y_i}{\partial x_3} \geq \left(\min_{k=21,34,65,78} |e_k| \right) \left(\min_{k=41,32,76,85} |e_k| \right) \left(\min_{k=51,62,73,84} |e_k| \right) \sin \alpha_i \cos \beta_i \stackrel{\text{def}}{=} J_i^m. \quad (2.63)$$

One useful concept is that of the flux across a face, inner or outer, defined by a fixed value of x_1 , x_2 or x_3 . For example, if we fix x_1 , the total flux across the face defined by this fixed value is

$$\int_{\Gamma_{x_1}} w_i \cdot n \, dS = \int_0^1 \int_0^1 w_i \cdot n \|\hat{n}\| \, dx_2 dx_3 = \int_0^1 \int_0^1 w_i \cdot \hat{n} \, dx_2 dx_3, \quad (2.64)$$

where n and \hat{n} are the normalized and non-normalized normal vectors, respectively, of Γ_{x_1} .

Finally, notice that

$$\sum_{l=1}^8 \phi_l = 1. \quad (2.65)$$

2.4.2 Three categories of hexahedra

The CVI behaves very differently on parallelepipeds, hexahedrons with planar faces, and hexahedrons with curved faces. Therefore a short treatment of these different hexahedra is appropriate.

With the assumption that the vertices are ordered in such a way that Ω_i is a non-degenerate hexahedron, and with some simple knowledge of the most basic properties of the trilinear mapping, one can divide the hexahedra, by properties of their faces, into three categories. The faces will be numbered in the following way:

Γ_{ij}	j
$x_1 = 0$	1
$x_1 = 1$	2
$x_2 = 0$	3
$x_2 = 1$	4
$x_3 = 0$	5
$x_3 = 1$	6

The faces of the reference cube, the normal vectors n_{ij} of the faces of Ω_i , the fluxes f_{ij} , and the shape functions ψ_{ij} will be numbered the same way. ψ_{ij} has flux one through the face Γ_{ij} and zero flux through the others.

If the vertices c_l of Ω_i fit a parallelepiped, then Ω_i is a parallelepiped. To prove this, we need the fact that the covariant vector are constants. We have

$$\begin{aligned} \frac{\partial y_i}{\partial x_1} = & -c_1(1-x_2)(1-x_3) + c_2(1-x_2)(1-x_3) + c_3x_2(1-x_3) \\ & -c_4x_2(1-x_3) - c_5(1-x_2)x_3 + c_6(1-x_2)x_3 + c_7x_2x_3 - c_8x_2x_3. \end{aligned} \quad (2.66)$$

Now in a hexahedron, there is a total of twelve edges between the eight vertices, and since the vertices are the vertices of a parallelepiped, four and four of these are identical. With our numbering of the vertices, this is made explicit through the equations

$$\begin{aligned} e_{21} = e_{34} = e_{65} = e_{78} = e_1 \\ e_{41} = e_{32} = e_{85} = e_{76} = e_2 \\ e_{51} = e_{62} = e_{73} = e_{84} = e_3, \end{aligned} \quad (2.67)$$

and when (2.67) is used in (2.66),

$$\begin{aligned} \frac{\partial y_i}{\partial x_1} &= e_{21}(1-x_2)(1-x_3) + e_{34}x_2(1-x_3) + e_{65}(1-x_2)x_3 + e_{87}x_2x_3 = \\ &e((1-x_2)(1-x_3) + x_2(1-x_3) + (1-x_2)x_3 + x_2x_3) = e_1. \end{aligned} \quad (2.68)$$

Similarly, we can compute

$$\frac{\partial y_i}{\partial x_2} = e_2 \quad \text{and} \quad \frac{\partial y_i}{\partial x_3} = e_3. \quad (2.69)$$

If the covariant vectors are constants, then n_{ij} will of course be constant on any outer face Γ_{ij} , and hence Γ_{ij} is planar. Since Ω_i then has planar outer faces and the vertices of a parallelepiped, it is a parallelepiped. With constant covariant vectors, the trilinear mapping can be written

$$y_i = Ax + b, \quad (2.70)$$

where $A = (e_1, e_2, e_3)$, and $b = c_1$ is the translation of the cell wrt the origin. A mapping which consists of a translation and a linear transformation is said to be affine.

We now proceed to describe Ω_i which are not a parallelepipeds, but in possession of planar outer faces. An outer face Γ_{ij} of Ω_i has four vertices, and if these four vertices lie in the same plane, then Γ_{ij} is planar. This is seen as follows. If the four corners of for instance Γ_{i2} lie in the same plane, then we have

$$\begin{aligned} e_{76} &= k_1e_{32} + k_2e_{62} \\ e_{73} &= k_3e_{32} + k_4e_{62}, \end{aligned} \quad (2.71)$$

for some k_1, k_2, k_3 , and k_4 . We compute the first component in (2.58),

$$\begin{aligned} &(e_{32}^2(1-x_3) + (k_1e_{32}^2 + k_2e_{62}^2)x_3)(e_{62}^3(1-x_2) + (k_3e_{32}^3 + k_4e_{62}^3)x_2) \\ &- (e_{32}^3(1-x_3) + (k_1e_{32}^3 + k_2e_{62}^3)x_3)(e_{62}^2(1-x_2) + (k_3e_{32}^2 + k_4e_{62}^2)x_2) = \\ &(e_{32}^2(1 + (k_1-1)x_3) + k_2e_{62}^2x_3)(e_{62}^3(1 + (k_4-1)x_2) + k_3e_{32}^3x_2) \\ &- (e_{32}^3(1 + (k_1-1)x_3) + k_2e_{62}^3x_3)(e_{62}^2(1 + (k_4-1)x_2) + k_3e_{32}^2x_2). \end{aligned} \quad (2.72)$$

When multiplied out, four of the terms cancel, leaving us with

$$\begin{aligned} &(e_{32}^2(1 + (k_1-1)x_3)e_{62}^3(1 + (k_4-1)x_2) + k_2e_{62}^2x_3k_3e_{32}^3x_2) \\ &(e_{32}^3(1 + (k_1-1)x_3)e_{62}^2(1 + (k_4-1)x_2) + k_2e_{62}^3x_3k_3e_{32}^2x_2) = \\ &e_{32}^2e_{62}^3[(1 + (k_1-1)x_3)(1 + (k_4-1)x_2) - k_2k_3x_2x_3] \\ &- e_{32}^3e_{62}^2[(1 + (k_1-1)x_3)(1 + (k_4-1)x_2) - k_2k_3x_2x_3] = \\ &(e_{32}^2e_{62}^3 - e_{32}^3e_{62}^2)[(1 + (k_1-1)x_3)(1 + (k_4-1)x_2) - k_2k_3x_2x_3]. \end{aligned} \quad (2.73)$$

Now similar arguments apply to the other components, giving

$$\begin{aligned} &\frac{\partial y_i}{\partial x_2} \times \frac{\partial y_i}{\partial x_3} = \\ &\left(\begin{array}{c} (e_{32}^2e_{62}^3 - e_{32}^3e_{62}^2) \\ (e_{32}^3e_{62}^1 - e_{32}^1e_{62}^3) \\ (e_{32}^1e_{62}^2 - e_{32}^2e_{62}^1) \end{array} \right) [(1 + (k_1-1)x_3)(1 + (k_4-1)x_2) - k_2k_3x_2x_3], \end{aligned} \quad (2.74)$$

which says that the normal vector always points in the same direction, implying the face to be planar. This does not imply planarity of inner faces defined by fixed values of x_1 , x_2 or x_3 .

Finally, note that if the corners of Γ_{ij} do not lie in the same plane, then obviously Γ_{ij} cannot be planar.

2.5 Velocity interpolation and mixed methods

As noted in the introduction, there are some key assumptions which, when satisfied, imply convergence of the mixed method. The inf-sup and coercivity conditions will be investigated for the CVI in section 3.2. These conditions depend on both of the approximation spaces Q_h and W_h . In sections 2.5.2 and 2.5.3 we explain briefly the problems that might be encountered with respect to these conditions. From now on, Q_h will be the space of constant pressures: let $q_i = \text{constant } \forall i$, and $Q_h = \{q; q|_{\Omega_i} = q_i \forall i\}$. All pressure-dependent considerations (except for section 2.5.3) and results below will be with respect to this space.

There is another important assumption made in the theorems of section 2.3, namely that $W_h \subseteq W$, and whether this is satisfied or not reduces to simple properties of the velocity field on each cell. This is explained in section 2.5.1.

2.5.1 The space $H(\text{div})$

Recall the definition of

$$W = H(\text{div}, \Omega) = \{w : (w)_k \in L^2(\Omega) \forall k; \text{div}(w) \in L^2(\Omega)\}, \quad (2.75)$$

and its norm

$$\|w\|_W = \sqrt{\sum_{k=1}^3 \|(w)_k\|_{L^2(\Omega)}^2 + \|\text{div}(w)\|_{L^2(\Omega)}^2}. \quad (2.76)$$

This is acknowledged as the correct space in which to seek velocity solutions of (2.14) and (2.15). The reasons for this are:

1. Its members have the sufficient regularity that all the integrands in (2.14) and (2.15) exist.
2. The components of w are members of $L^2(\Omega)$, which ensures that the integrals in (2.14) and (2.15) are finite.
3. They admit a certain degree of discontinuity, which is demanded by the discontinuous permeability matrix and Darcy's law.

When finding approximations to these solutions, we would obviously like the approximations to belong to the same space as the exact solutions. That is, we would like to have $W_h \subseteq W$. There are two conditions which together imply that $w \in W_h$ is a member of W :

1. The components of w or $\text{div}(w)$ are members of $L^2(\Omega)$.
2. $\text{div}(w)$ exists in the weak sense, and is a member of $L^2(\Omega)$.

The first condition is never a problem, because nobody would construct a velocity interpolation whose components were not in $L^2(\Omega)$. The second condition, however, is quite important. That the components of w itself are members of $L^2(\Omega)$ does not demand anything of the continuity; w may have discontinuities across any face in the decomposition of Ω . But $\text{div}(w)$ is to be understood in the weak sense, and this has implications on the continuity of $w \cdot n$ across any face of discontinuity, because the weak divergence will not exist if the velocity is not continuous in the normal direction across any such face. We omit the proof, but the argument is as follows: in the space of smooth functions $C^\infty(\Omega)$, the Green's formulas hold. It is possible to show that W is dense in $C^\infty(\Omega)$

wrt. the W -norm, and this implies that Green's formulas also hold in W . With Green's formulas, it is easy to prove that any function in W has to be continuous in the normal direction across any face of discontinuity. The proof of this last statement can be found in [1], p. 23-25. See also [11]. See [8], p. 242 for the definition of weak derivatives. The scalar field $w \cdot n$ is commonly called the normal trace.

An analogy is the standard example, which can be found in [8] p. 243-244, of the function $f(x) = |x|$. This function has the Heaviside function as its weak derivative. However, the function

$$g(x) = \begin{cases} 2 - x & x < 0 \\ 1 + x & x \geq 0 \end{cases}$$

does not have a weak derivative, even though its classical derivative is identical with the classical derivative of f wherever these are defined. The weak derivative is thus allowed to have discontinuities, but not the function itself, if it is to have a weak derivative. It is the same phenomenon with functions in W ; the divergence is allowed to be discontinuous, but a continuity restriction necessary for the existence of the weak divergence holds for the function itself.

Mass conservation and $H(\text{div})$

The degrees of freedom of the velocity space are often net fluxes across the faces of the grid, and the velocity interpolation w_i on each cell Ω_i is obtained by taking a linear combination of the six shape functions ψ_{ij} of that cell and the fluxes f_{ij} of its faces:

$$w_i = \sum_{j=1}^6 f_{ij} \psi_{ij}. \quad (2.77)$$

(Recall that ψ_{ij} has flux one through Γ_{ij} and zero through the five others.) If we have specified a flux f_{ij} across a certain face Γ_{ij} in order to construct w_i , then obviously we should expect w_i to reproduce this flux correctly; in other words that

$$\int_{\Gamma_{ij}} w_i \cdot n \, dS = f_{ij}. \quad (2.78)$$

The interpolation is then said to be mass conservative.

Aside from the fact that this is a very natural property to demand of w_i , there is also a very important reason. If the interpolation does not reproduce fluxes correctly, there is no guarantee that the flux of a face Γ is reproduced identically in the two different cells sharing Γ , and then it is not possible to guarantee continuity of the normal trace across Γ . Assume we have two cells Ω_1 and Ω_2 with respective velocity interpolations w_1 and w_2 , sharing a face Γ . If

$$\int_{\Gamma} w_1 \cdot n \, dS \neq f_{\Gamma} \neq \int_{\Gamma} w_2 \cdot n \, dS, \quad (2.79)$$

then we cannot expect to have

$$\int_{\Gamma} w_1 \cdot n \, dS = \int_{\Gamma} w_2 \cdot n \, dS, \quad (2.80)$$

and hence we cannot guarantee continuity of $w \cdot n$ across Γ . More specifically, if $\int_{\Gamma_j} w_1 \cdot n \, dS$ and $\int_{\Gamma_j} w_2 \cdot n \, dS$ depend on the shape functions ψ_{1k} and ψ_{2k} for $k \neq j$, then the value of these integrals can be varied independently of each other, and normal continuity is obviously impossible.

Recall the bilinear form $b(q, w) = \int_{\Omega} q \, \text{div}(w) \, dy$, defined in (2.18). We define the restriction of $b(\cdot, \cdot)$ to Ω_i :

$$b_i(q, w) = \int_{\Omega_i} q_i \, \text{div}(w_i) \, dy. \quad (2.81)$$

If a method reproduces the correct fluxes, then for our choice of Q_h we have

$$b_i(q, w) = q_i \int_{\Omega_i} \operatorname{div}(w_i) dy = q_i \int_{\partial\Omega_i} w_i \cdot n dS = q_i \sum_{j=1}^6 f_{ij}, \quad (2.82)$$

and hence

$$b(q, w) = \sum_i q_i \int_{\Omega_i} \operatorname{div}(w_i) dy = \sum_i q_i \sum_{j=1}^6 f_{ij}, \quad (2.83)$$

so the space $Z_h = \{w \in W_h : b(q, w) = 0 \forall q \in Q_h\}$ is the space of all $w_h \in W_h$ with no accumulation of mass in any cell in the grid.

Reproduction of uniform flow and $H(\operatorname{div})$

Whenever we compute anything, we would like our formulas to be mathematically exact for as many of the simplest cases as possible. One example is Gauss quadrature integration formulas which, under the freedom of choosing n nodes and n coefficients, are exact for polynomials of degree $2n + 1$. As uniform flow is probably the simplest case there is, we would prefer that our mathematical formulas actually produce uniform flow if this is the correct physical solution. It is important realizing here that if we say that a method reproduces uniform flow, then the approximation formulas simplify to the constant flow field mathematically, i.e. it is possible to prove that a constant w_0 results if the method is applied to a case where uniform flow is the correct solution.

Definition 2.5.1 *The fluxes of Ω are said to be uniform-flow-consistent with w_0 if there exists a constant w_0 such that*

$$f_{ij} = \int_{\Gamma_j} w_0 \cdot n dS \quad j = 1, \dots, 6. \quad (2.84)$$

Definition 2.5.2 *A velocity interpolation is said to reproduce uniform flow on Ω_i if the interpolated velocity w simplifies to w_0 on Ω_i whenever the fluxes of Ω_i are uniform flow consistent with w_0 .*

In the case of curved Γ , the property of reproducing uniform flow is conflicting with the continuity of $w \cdot n$ across Γ . This can be illustrated by the following construction. Consider two cells Ω_1 and Ω_2 sharing a face Γ_j , with given, *constant* velocity interpolations w_1 and w_2 , respectively. Let w_1 and w_2 determine the fluxes of Ω_1 and Ω_2 . There is now one constraint:

$$\int_{\Gamma_j} w_1 \cdot n_{1j} dS = \int_{\Gamma_j} w_2 \cdot n_{2j} dS, \quad (2.85)$$

since the flux is associated with the face and has to be the same evaluated in Ω_1 and Ω_2 . Aside from this constraint, w_1 and w_2 can be chosen freely. If now Γ is planar, then one sees easily that the normal continuity is automatically satisfied in this case, so reproduction of uniform flow is not incompatible with normal continuity if Γ is planar. But if Γ is not planar, then we have to compare the quantities $w_1 \cdot n$ and $w_2 \cdot n$ when n is not constant, and these expressions will not equal in general unless $w_1 = w_2$. This implies that it is possible to construct examples for which a uniform-flow-reproducing method would necessarily have a discontinuous normal trace, and hence such a method would not produce a global velocity in W . See [12] for a proof of this.

2.5.2 The coercivity condition

Recall from the preceding chapter that the velocity part of the solution of a mixed method is stable if the bilinear form $a(\cdot, \cdot)$ is coercive on the space $Z_h = \{w \in W_h : b(q, w) = 0 \forall q \in Q_h\}$. One way to guarantee this, is to demand that $Z_h \subseteq Z$; which is sufficient since it is possible to prove that $a(\cdot, \cdot)$ is coercive on the space Z . Since Z is the divergence free subspace of W , this amounts to choosing the degrees of freedom of the velocity in such a way that the divergence is identically zero for all functions in Z_h . Recall that when Q_h is the space of constant pressures, then Z_h is the space of all $w_h \in W_h$ with no net accumulation of mass in any cell, so we should demand that the divergence is the zero function on each Ω_i as long as the fluxes f_{ij} of Ω_i sum to zero.

If this is not the case, then we might have trouble with the coercivity on grids which do not become increasingly uniform as they are refined. To get a feel for what might go wrong, consider the following example. Let $f_h(x)$ denote the linear interpolation between two independent values $f_1(0)$ and $f_2(h)$ on the interval $(0, h)$ on the real axis. If we let $h \rightarrow 0$, and specify $f_1(0) = 1/h$, $f_2(h) = 4/h$, then f_h will grow as $1/h$, while its derivative with respect to x will grow as $1/h^2$.

A related phenomenon might happen if $Z_h \not\subseteq Z$. Consider the so-called 'truncated pyramid', depicted in fig 2.3 below.

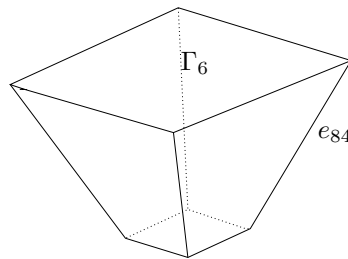


Figure 2.3: Truncated pyramid. The edges e_{51} , e_{62} , e_{73} , and e_{84} protrude from the face Γ_5 with the same angle. The faces Γ_5 and Γ_6 are parallel.

This cell has as its main characteristics that two opposite outer faces, for example Γ_5 and Γ_6 , are parallel squares, and the four other faces protrude from the plane of Γ_5 with the same angle of $3\pi/4$. If we set $f_5 = -1$, $f_6 = 1$, and the other fluxes to zero, then a mass conservative velocity interpolation on this cell is a member of Z_h on this 'grid', which consists of only one cell. With an angle of $3\pi/4$, the face Γ_5 has side h , and Γ_6 has side $2h$. We now let $h \rightarrow 0$ while the fluxes remain fixed. In order to integrate to the correct fluxes, the strength of the component along the x_3 -direction of the velocity interpolation will become unbounded as $h \rightarrow 0$, and the strength at Γ_5 will be four times bigger than at Γ_6 , since the area of Γ_5 is exactly one fourth of Γ_6 . This means that while the function values of and their differences grow as $1/h^2$, the derivative in the same direction will grow as

$$\frac{3/h^2}{1/h} = 3/h^3, \quad (2.86)$$

which is of one order more than the function values.

Recall that the coercivity condition depends on the W -norm of the velocity. Since this is dependent on the divergence, which is again dependent on this $1/h^3$ derivative, then the divergence norm might grow considerably faster as $h \rightarrow 0$ than the right hand side, which is just a weighted $L_2(\Omega)^3$ -norm, and thus we cannot expect the coercivity condition to be satisfied as $h \rightarrow 0$ with an α which is bounded away from zero.

The problem in this example was the insistence on keeping the shape of the truncated pyramid as the 'grid' was refined. This is what made the derivative grow as $1/h^3$. There are two obvious

things that could be done to prevent this. If we instead let the cell become congruent to the cube with edges h as $h \rightarrow 0$, then the difference in the numerator in (2.86) would approach zero, dampening the growth of the derivative. The other thing that could be done, is ensuring that $Z_h \subseteq Z$, for the W -norm depends on the divergence, and if this is zero on Z_h , then the individual derivatives could be allowed to grow arbitrarily without this affecting the norm.

2.5.3 The inf-sup condition

The coercivity condition determines the stability of v_h as the grid is refined. The stability of p_h is determined by both the coercivity and inf-sup conditions. While there is usually no problem to find a coercivity constant α_h for each grid; the only issue is determining whether this constant is independent of the grid, for the inf-sup condition there might even be no constant β_h such that the condition is satisfied for any grid. A simple example is to consider a case with linear velocity and polynomial pressure approximation space of order greater than zero on each cell. The divergence space of W_h then contains only constants, and if we choose q_h with

$$\int_{\Omega_i} q_h dy = 0 \quad (2.87)$$

for all Ω_i , then obviously the inf-sup condition cannot be satisfied on any grid.

2.5.4 Example: The space RT_0

A simple family of mixed finite element spaces are the Raviart-Thomas spaces. In the next chapter, we will need the simplest of these spaces, which is called RT_0 . On the reference element, this space is ([7], p.128)

$$RT_0 = W_h = \{w_K : w_K = (a_1x_1 + b_1, a_2x_2 + b_2, a_3x_3 + b_3)\}, \quad (2.88)$$

where w_K is used to indicate that the velocity is on the reference element. For general elements, this space on K is mapped to physical space by the Piola transformation P_i ([1] p. 135)

$$w_i = P_i w_K, \quad (2.89)$$

where

$$P_i = \frac{1}{J_i} \frac{dy_i}{dx}. \quad (2.90)$$

Note that w is still a function of the reference variable x .

If the cell Ω_i in physical space is a parallelepiped, then from (2.60), we have

$$\frac{dy_i}{dx} = (e_1, e_2, e_3), \quad (2.91)$$

and

$$J_i = e_1 \cdot e_2 \times e_3 = |e_1||e_2||e_3| \sin \theta_1 \cos \theta_2 = |e_1| \cos \theta_2 A_{i2}. \quad (2.92)$$

Since Ω_i is a parallelepiped, θ_2 is here the angle between n_2 and e_1 . Note that these equations could have been written in many ways, depending on which way to write the Jacobian determinant. It is easy to check by using (2.89) and (2.92), that for example

$$\psi_{i2} = \frac{e_{21}}{|e_{21}| A_2 \cos \theta_2} x_1, \quad (2.93)$$

for the RT_0 space.

Chapter 3

Analysis of the corner velocity interpolation (CVI)

'Interpolasjon? Ka skulle vi gjort uten?'

Terje O. Espelid

3.1 Construction of the interpolation and assembly of its basic properties

This section constructs the corner velocity interpolation and assembles some of its important properties. The question of whether the CVI could be used as the space W_h in a mixed method is addressed in section 3.2, by considering how it does and does not satisfy the inf-sup and coercivity conditions.

3.1.1 The CVI on cells with planar outer faces

In the following, we will assume planar outer faces, as the construction of the CVI method and assembly of its properties on general hexahedra, should be seen in light of this simple case. The original formulation of the method may be found in [9]. In this chapter, when we write w_i , we shall always mean $w_i = w_i^{CVI}$. Similarly, W_h always means $W_h = W_h^{CVI}$.

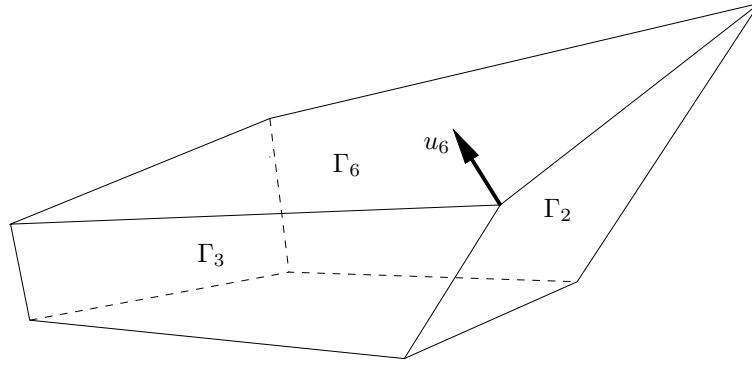
To construct the CVI on Ω_i , first compute eight bulk Darcy velocities u_l , one for each corner c_l of Ω_i . This is done by solving eight 3×3 linear sets of equations

$$u_l \cdot n_{ij} = f_{ij}/A_{ij} \quad l = 1, \dots, 8. \quad (3.1)$$

For each l , the index j ranges over the three outer faces sharing the vertex c_l , giving three equations for each u_l . When these eight corner velocities have been computed, one builds an interpolation with the ϕ 's of the trilinear mapping,

$$w_i(x) = \sum_{l=1}^8 u_l \phi_l(x), \quad (3.2)$$

and this gives a velocity field on the parametric form described in the beginning of section 2.4.

Figure 3.1: The corner velocity u_l

The eight 3×3 linear systems for the eight u_l 's may be written:

$$N_l u_l = F_l, \quad (3.3)$$

where the rows of N_l are the three normal vectors n_{l1} , n_{l2} and n_{l3} associated with the corner c_l , and F_l consists of the three corresponding ratios between flux and area. We have

$$\det N_l = n_{l1} \cdot (n_{l2} \times n_{l3}), \quad (3.4)$$

so if we want a unique solution, we must have

$$n_{l1} \cdot (n_{l2} \times n_{l3}) \neq 0 \quad \text{for } l = 1, \dots, 8. \quad (3.5)$$

According [2], p. 616, this is the case if and only if the three vectors n_{l1} , n_{l2} and n_{l3} are not coplanar. Coplanarity of n_{l1} , n_{l2} and n_{l3} obviously corresponds to a degeneration of the cell, so this will not be considered.

Remark 3.1.1 Note that each corner velocity, when multiplied with one of its three normal vectors and integrated over the corresponding face, gives back the correct flux of the face:

$$\int_{\Gamma} u_l \cdot n dS = u_l \cdot n \int_{\Gamma} dS = \frac{f_{\Gamma}}{A_{\Gamma}} A_{\Gamma} = f_{\Gamma}. \quad (3.6)$$

Theorem 3.1.1 On hexahedra with planar outer faces, we have:

1. $w_i \cdot n$ is constant on outer faces.
2. w_i reproduces the correct face fluxes.
3. $w_i \cdot n$ is continuous across a face shared by two cells.
4. w_i reproduces uniform flow according to definition (2.5.2).

Proof: 1. For example, for the face Γ_{i2} ,

$$\begin{aligned} w_i \cdot n_{i2} &= \left(\sum_{l=1}^8 u_l \phi_l(1, x_2, x_3) \right) \cdot n_{i2} = \\ &= u_2 \cdot n_{i2}(1-x_2)(1-x_3) + u_3 \cdot n_{i2}x_2(1-x_3) + u_6 \cdot n_{i2}(1-x_2)x_3 + u_7 \cdot n_{i2}x_2x_3 = \\ &= f_{i2}/A_{i2}(1-x_2)(1-x_3) + f_{i2}/A_{i2}x_2(1-x_3) + f_{i2}/A_{i2}(1-x_2)x_3 + f_{i2}/A_{i2}x_2x_3 = \\ &= f_{i2}/A_{i2}((1-x_2)(1-x_3) + x_2(1-x_3) + (1-x_2)x_3 + x_2x_3) = f_{i2}/A_{i2}. \end{aligned} \quad (3.7)$$

The computations are similar for the other five outer faces.

2. Consider the integral (2.64) when Γ_{ij} is an outer face,

$$\int_{\Gamma_{ij}} w_i \cdot n_{ij} dS = \int_{\Gamma_{ij}} f_{ij}/A_{ij} dS = f_{ij}/A_{ij} \int_{\Gamma_{ij}} dS = f_{ij}. \quad (3.8)$$

3. Let Ω_1 and Ω_2 be hexahedra with CVI velocity fields $w_1(x)$ and $w_2(x)$, respectively, sharing a planar face Γ . Because of property 1., we have at Γ

$$w_1 \cdot n_\Gamma = f_\Gamma/A_\Gamma = w_2 \cdot n_\Gamma, \quad (3.9)$$

which shows normal continuity.

4. If the fluxes f_{ij} of Ω_i are uniform flow consistent with w_0 , then

$$f_{ij} = \int_{\Gamma_{ij}} w_0 \cdot n_{ij} dS = w_0 \cdot n_{ij} A_{ij}, \quad (3.10)$$

for $j = 1, \dots, 6$. When plugged into (3.1), this gives

$$u_l \cdot n_{ij} = f_{ij}/A_{ij} = w_0 \cdot n_{ij}, \quad (3.11)$$

where j again ranges over the three faces sharing c_l . This system obviously has the unique solution $u_l = w_0$, and as this argument was independent of the corner in question, we have $u_l = w_0$ for all $l = 1, \dots, 8$. But then

$$w_i = \sum_{l=1}^8 u_l \phi_l = \sum_{l=1}^8 w_0 \phi_l = w_0 \sum_{l=1}^8 \phi_l = w_0, \quad (3.12)$$

as conjectured. \square

Remark 3.1.2 *Note that the CVI, since it reproduces uniform flow, is coercive on the subspace of uniform-flow-consistent fluxes.*

Construction of shape function

We now construct the CVI shape function. We will construct the shape function ψ_{i2} only; the other constructions are similar.

Consider a cell Ω_i with flux one through Γ_{i2} , and zero fluxes through all other faces. The CVI for this cell is

$$\psi_{i2}(x) = x_1 (u_2(1-x_2)(1-x_3) + u_3x_2(1-x_3) + u_6(1-x_2)x_3 + u_7x_2x_3) / A_{i2}. \quad (3.13)$$

Here $u_2 = \frac{t_{21}}{\cos \theta_2}$, θ_2 is the angle between n_2 and t_{21} , and the expressions for u_3 , u_6 , and u_7 are similar. It is then easily checked that ψ_{i2} has flux one through Γ_{i2} , and zero flux through the other faces. Expression (3.13) enables us to write

$$w_i = \sum_{l=1}^8 u_l \phi_l(x) = \sum_{j=1}^6 f_{ij} \psi_{ij}(x), \quad (3.14)$$

which will be useful in the following, as it displays the six degrees of freedom in an obvious way, as opposed to (3.2).

In the special case of parallelepipeds, (3.13) simplifies to

$$\psi_{i2} = \frac{t_{21}}{A_{i2} \cos \theta_2} x_1 = \frac{e_1}{|e_1| A_{i2} \cos \theta_2} x_1, \quad (3.15)$$

since the edges e_{21} , e_{34} , e_{65} , and e_{78} are parallell. Similar computations hold for the other shape functions ψ_{ij} . We have thus

Theorem 3.1.2 *If Ω_i is a parallelepiped, then the CVI interpolation is identical to the interpolation of the RT_0 space.*

Proof: Compare with (2.93). \square

3.1.2 The CVI on cells with curved outer faces

Let us now construct the CVI method for general hexahedra curved faces. Recall that our construction involved two steps; extraction of corner velocities and assembly of formula (3.2). The second part is done in the same way, and computing the corner velocities when Γ_{ij} does not have a constant normal vector is done in the following way. First define the average of the normal vector of Γ_{ij}

$$\bar{n}_{ij} = \int_{\Gamma_{ij}} n_{ij} dS, \quad (3.16)$$

then solve, as in the the planar case,

$$u_l \cdot \bar{n}_{ij} = f_{ij}. \quad (3.17)$$

This evidently still gives the eight linear systems to solve for the u_l 's. Note that when Γ_{ij} is planar, then $\bar{n}_{ij} = n_{ij}$, and (3.17) simplify to (3.1).

Lemma 3.1.3 *The CVI reproduces uniform flow according to definition (2.5.2) on hexahedra with curved faces.*

Proof: The argument is identical to that of the planar case, but with the additional fact that for uniform w_0

$$\int_{\Gamma_{ij}} w_0 \cdot n_{ij} dS = w_0 \cdot \int_{\Gamma_{ij}} n_{ij} dS = w_0 \cdot \bar{n}_{ij} A_{ij}, \quad (3.18)$$

for $j = 1, \dots, 6$. \square

Lemma 3.1.4 *If Γ_{ij} is curved, then for the CVI we do not have*

$$\int_{\Gamma_{ij}} w_i \cdot n dS = f_{ij} \quad (3.19)$$

in general.

Proof: We will demonstrate this by computing a counter example. The shape function ψ_2 (we drop the subscript i for this example) is

$$\psi_2(x) = u_2 x_1 (1 - x_2) (1 - x_3) + u_3 x_1 x_2 (1 - x_3) + u_6 x_1 (1 - x_2) x_3 + u_7 x_1 x_2 x_3. \quad (3.20)$$

The quantities u_l can be made explicit in a similar way to the planar-face case, but we omit the details. For this shape function ψ_2 , we should have

$$\int_{\Gamma_2} \psi_2 \cdot n dS = 1, \quad (3.21)$$

and

$$\int_{\Gamma_j} \psi_2 \cdot n dS = 0, \quad (3.22)$$

for $j = \{1, 3, 4, 5, 6\}$. Now consider a cell with corners

c_l	y
c_1	$(0, 0, 0)$
c_2	$(1, 0, 0)$
c_3	$(1, 1, 0)$
c_4	$(0, 1, 0)$
c_5	$(0, 0, 1)$
c_6	$(1, 0, 1)$
c_7	$(2, 2, 2)$
c_8	$(0, 1, 1)$

Let us compute the flux through the face Γ_6 . We have then

$$\psi_2(x_1, x_2, 1) = u_6 x_1(1 - x_2) + u_7 x_1 x_2. \quad (3.23)$$

To compute u_6 and u_7 , we need the normal vectors \bar{n}_2 , \bar{n}_3 , \bar{n}_4 , and \bar{n}_6 . These are

$$\begin{aligned} \bar{n}_2 &= (2, -1/2, -1/2), \\ \bar{n}_3 &= (0, -1, 0), \\ \bar{n}_4 &= (-1/2, 2, -1/2), \\ \bar{n}_6 &= (-1/2, -1/2, 2). \end{aligned} \quad (3.24)$$

Now q_6 defined by

$$\begin{aligned} u_6 \cdot n_2 &= 1, \\ u_6 \cdot n_3 &= 0, \\ u_6 \cdot n_6 &= 0, \end{aligned} \quad (3.25)$$

and a similar set of equations for u_7 , gives

$$\begin{aligned} u_6 &= (8/15, 0, 2/15), \\ u_7 &= (3/5, 1/5, 1/5), \end{aligned} \quad (3.26)$$

or

$$\psi_2(x_1, x_2, 1) = x_1(8/15 + x_2/15, x_2/5, 2/15 + x_2/15). \quad (3.27)$$

The unit normal vector of Γ_6 is, as in (2.58),

$$\hat{n}_6 = (-x_2, -x_1, 1 + x_1 + x_2). \quad (3.28)$$

We then compute

$$\int_{\Gamma_6} \psi_2 \cdot n \, dS = \frac{1}{180}, \quad (3.29)$$

which is not the specified flux of Γ_6 . \square

Corollary 3.1.1 *For the CVI on grids with curved faces, we do not have $W_h \subseteq W$ in general.*

Proof: This follows both from the reproduction of uniform flow and the non-reproduction of correct fluxes. See section 2.5.1. \square

Remark 3.1.3 We do know, however, that

$$\int_{\Gamma} w \cdot \bar{n} dS = f_{\Gamma}, \quad (3.30)$$

but this does not help us, as in general

$$\int_{\Gamma} w \cdot \bar{n} dS \neq \int_{\Gamma} w \cdot n dS, \quad (3.31)$$

unless w is constant. Note that this implies that the CVI reproduces the fluxes correctly in the case of uniform flow.

Remark 3.1.4 Lemma 3.1.3 is not all there is to say about reproduction of correct fluxes on curved faces; there are exceptions to this rule. Consider the following cell,

c_l	y
c_1	$(a_1, 0, 0)$
c_2	$(a_2, 0, 0)$
c_3	$(a_3, 1, 0)$
c_4	$(a_4, 1, 0)$
c_5	$(a_5, 0, 1)$
c_6	$(a_6, 0, 1)$
c_7	$(a_7, 1, 1)$
c_8	$(a_8, 1, 1)$

with $a_1 < a_2$, $a_4 < a_3$, $a_5 < a_6$, and $a_8 < a_7$, to secure a consistent numbering of the corners, and non-degeneration of the cell. The edges e_{21} , e_{34} , e_{65} , and e_{78} of this cell are parallel, and this implies, through a simple computation, that the fluxes of the two non-planar faces Γ_1 and Γ_2 are reproduced correctly: (cf. (3.15))

$$\int_{\Gamma_2} \psi_2 \cdot n dS = \frac{1}{A_2} \int_{\Gamma_2} dS = 1. \quad (3.32)$$

The computation for ψ_1 is identical.

Remark 3.1.5 The reproduction of uniform flow implies that the CVI cannot have constant normal components on curved outer faces, since $w_0 \cdot n$ is not a constant when w_0 is constant and n is not. There is a component of the CVI which is constant on outer faces, namely the component along \bar{n}_{ij} , which is seen easily when multiplying with \bar{n}_{ij} of a certain face and evaluating at this face.

3.1.3 The divergence of the CVI

The divergence of the CVI is of interest to us for two reasons:

1. We are modelling incompressible flow, so we would like the divergence to equal zero pointwise on cell interiors if the face fluxes add to zero. The velocity interpolation is then said to be divergence free.

2. If the divergence is the zero function for such fluxes, then we would have $Z_h \subseteq Z$, which would imply coercivity of the CVI together with the space Q_h of constant pressures in the mixed method. See section 2.5.1.

We are of course interested in the divergence wrt. the physical coordinates y . There is no explicit formula for the CVI as a function of y , but the divergence wrt. y can be computed via the chain rule.

$$\begin{aligned} \frac{dw_i}{dx} &= \frac{dw_i}{dy} \frac{dy_i}{dx} \quad \implies \\ \frac{dw_i}{dy} &= \frac{dw_i}{dx} \left(\frac{dy_i}{dx} \right)^{-1} \quad \implies \\ \operatorname{div}_y w_i &= \operatorname{tr} \left(\frac{dw_i}{dx} \left(\frac{dy_i}{dx} \right)^{-1} \right). \end{aligned} \quad (3.33)$$

Written out, this becomes

$$\operatorname{div}_y w_i = \frac{\frac{\partial w_i}{\partial x_1} \cdot \frac{\partial y_i}{\partial x_2} \times \frac{\partial y_i}{\partial x_3} + \frac{\partial w_i}{\partial x_2} \cdot \frac{\partial y_i}{\partial x_3} \times \frac{\partial y_i}{\partial x_1} + \frac{\partial w_i}{\partial x_3} \cdot \frac{\partial y_i}{\partial x_1} \times \frac{\partial y_i}{\partial x_2}}{J}. \quad (3.34)$$

Corollary 3.1.2 *For the CVI on grids with only planar faces, we have $W_h \subseteq W$.*

Proof: Evidently, w_i and $\operatorname{div}_y w_i$ are bounded on each Ω_i , and the normal trace is continuous across all faces in the grid. \square

Lemma 3.1.5 *For the CVI, we do not have $Z_h \subseteq Z$ on general Ω_i .*

Proof: Consider again the truncated pyramid of fig. 2.3, with fluxes $f_j = 0$ for $j = 1, 2, 3, 4$, $f_5 = -1$ and $f_6 = 1$. The fluxes add to zero, so we just have to check the divergence function (3.33). We recall the construction of the shape functions ψ_{ij} at the end of section 3.1.1, and compute for this truncated pyramid:

$$\begin{aligned} w_i &= -\psi_{i5} + \psi_{i6} = \\ & \left(\frac{1-x_3}{A_{i5}} + \frac{x_3}{A_{i6}} \right) (t_{51}(1-x_1)(1-x_2) + t_{62}x_1(1-x_2) + t_{73}x_1x_2 + t_{84}(1-x_1)x_2) / \cos \theta_i, \end{aligned} \quad (3.35)$$

$$(3.36)$$

and for a general truncated pyramid

$$\begin{aligned} \frac{dy_i}{dx_1} &= e_{21}(1 + (k-1)x_3), \\ \frac{dy_i}{dx_2} &= e_{41}(1 + (k-1)x_3), \\ \frac{dy_i}{dx_3} &= e_{51}(1-x_1)(1-x_2) + e_{62}x_1(1-x_2) + e_{73}x_1x_2 + e_{84}(1-x_1)x_2, \end{aligned} \quad (3.37)$$

where k is the scaling factor between the sides of Γ_5 and Γ_6 . Now choose a specific truncated pyramid with corners

c_l	y
c_1	$(1, 1, 0)$
c_2	$(2, 1, 0)$
c_3	$(2, 2, 0)$
c_4	$(1, 2, 0)$
c_5	$(0, 0, 1)$
c_6	$(3, 0, 1)$
c_7	$(3, 3, 1)$
c_8	$(0, 3, 1)$

When this is plugged into (3.35) and (3.37), respectively, we get

$$\frac{dw_i}{dx} = \begin{pmatrix} 2 - 16x_3/9 & 0 & 8/9(1 - 2x_1) \\ 0 & 2 - 16x_3/9 & 8/9(1 - 2x_2) \\ 0 & 0 & -8/9 \end{pmatrix},$$

and

$$\frac{dy_i}{dx} = \begin{pmatrix} 1 + 2x_3 & 0 & 2x_1 - 1 \\ 0 & 1 + 2x_3 & 2x_2 - 1 \\ 0 & 0 & 1 \end{pmatrix}.$$

The inverse of $\frac{dy_i}{dx}$ is

$$\left(\frac{dy_i}{dx}\right)^{-1} = \frac{1}{(1 + 2x_3)^2} \begin{pmatrix} 1 + 2x_3 & 0 & (1 + 2x_3)(1 - 2x_1) \\ 0 & 1 + 2x_3 & (1 + 2x_3)(1 - 2x_2) \\ 0 & 0 & (1 + 2x_3)^2 \end{pmatrix}.$$

We now let matlab compute

$$\operatorname{div}_y w_i = \operatorname{tr} \left(\frac{dw_i}{dx} \left(\frac{dy_i}{dx}\right)^{-1} \right) = \frac{(28/9 + 8/9x_3 - 32/3x_3^2)}{(1 + 2x_3)^2} \neq 0, \quad (3.38)$$

and we conclude that the CVI is not in general divergence free on non-parallellepiped Ω_i . \square

3.1.4 Local estimates for the CVI

In order to discuss the CVI as an approximation space for the velocity in a mixed method, we need some bounds for the W -norm, starting with a local bound. In this section $(\cdot)_k$ always means the k 'th component. First recall the W -norm of the CVI on Ω_i

$$\|w_i\|_W = \sqrt{\sum_{k=1}^3 \|(w_i)_k\|_{L^2(\Omega_i)}^2 + \|\operatorname{div}(w_i)\|_{L^2(\Omega_i)}^2}. \quad (3.39)$$

Bounding the L^2 -norm of the components is straightforward. We have

$$|(w_i)_k| = \left| \sum_{j=1}^6 f_{ij}(\psi_{ij})_k \right| \leq \sum_{j=1}^6 |f_{ij}| |(\psi_{ij})_k|, \quad (3.40)$$

and bounding ψ_{ij} can be done the following way. For example, for $(\psi_2)_k$:

$$|(\psi_2)_k| = |x_1((w_2)_k(1 - x_2)(1 - x_3) + (w_3)_k x_2(1 - x_3) + (w_6)_k(1 - x_2)x_3 + (w_7)_k x_2 x_3) / A_2| \leq \quad (3.41)$$

$$x_1 (|(q_2)_k|(1 - x_2)(1 - x_3) + |(q_3)_k|x_2(1 - x_3) + |(q_6)_k|(1 - x_2)x_3 + |(q_7)_k|x_2 x_3) / A_2 \leq$$

$$x_1 \max_{l=2,3,6,7} \frac{1}{A_2} |(q_l)_k| \leq \frac{1}{A_2} \max_{l=2,3,6,7} \frac{1}{\cos \theta_l} = B_{i2}.$$

The bounds for the other ψ_{ij} 's are similar. If we denote by f_{im} the absolute value of the largest of the six fluxes, and by B_{im} the largest of the six B_{ij} , then

$$|(w_i)_k| \leq 6f_{im}B_{im}. \quad (3.42)$$

As for the L^2 -norm of the divergence, given in eq. (3.34), we have

$$\begin{aligned} |\operatorname{div}_y(w_i)| &\leq \\ \frac{|\frac{\partial w_i}{\partial x_1} \cdot \frac{\partial y_i}{\partial x_2} \times \frac{\partial y_i}{\partial x_3}| + |\frac{\partial w_i}{\partial x_2} \cdot \frac{\partial y_i}{\partial x_3} \times \frac{\partial y_i}{\partial x_1}| + |\frac{\partial w_i}{\partial x_3} \cdot \frac{\partial y_i}{\partial x_1} \times \frac{\partial y_i}{\partial x_2}|}{J} &\leq \\ \frac{|\frac{\partial w_i}{\partial x_1}| \|\frac{\partial y_i}{\partial x_2}\| \|\frac{\partial y_i}{\partial x_3}\| + |\frac{\partial w_i}{\partial x_2}| \|\frac{\partial y_i}{\partial x_3}\| \|\frac{\partial y_i}{\partial x_1}\| + |\frac{\partial w_i}{\partial x_3}| \|\frac{\partial y_i}{\partial x_1}\| \|\frac{\partial y_i}{\partial x_2}\|}{J} &\leq \\ \frac{|e_m|^2}{J_i^m} \left(\left| \frac{\partial w_i}{\partial x_1} \right| + \left| \frac{\partial w_i}{\partial x_2} \right| + \left| \frac{\partial w_i}{\partial x_3} \right| \right), & \end{aligned} \quad (3.43)$$

where e_m is the longest edge of Ω_i and we have employed (2.63) to get J_i^m . The $|\frac{\partial w_i}{\partial x_k}|$ we can bound in ways similar to the components of the CVI:

$$\left| \frac{\partial w_i}{\partial x_k} \right| = \left| \frac{\partial \sum_j f_{ij} \psi_{ij}}{\partial x_k} \right| = \left| \sum_j f_{ij} \frac{\partial \psi_{ij}}{\partial x_k} \right| \leq f_{im} \sum_j \left| \frac{\partial \psi_{ij}}{\partial x_k} \right|. \quad (3.44)$$

The term $\sum_j \left| \frac{\partial \psi_{ij}}{\partial x_k} \right|$ is only dependent on the cell's geometry, and hence is bounded by a constant D dependent only on this geometry, giving

$$|\operatorname{div}_y(w_i)| \leq 3D \frac{|e_m|^2 f_{im}}{J_i^m}. \quad (3.45)$$

Using all this in (3.39) gives

$$\begin{aligned} \|w_i\|_W &= \sqrt{\sum_k \|(w_i)_k\|_{L^2(\Omega_i)}^2 + \|\operatorname{div}(w)\|_{L^2(\Omega_i)}^2} \leq \\ \sqrt{V_{\Omega_i} \left(3 \cdot (6f_{im}|B_{im}|)^2 + (D \frac{|e_m|^2 f_{im}}{J_i^m})^2 \right)} &= C_i f_{im}, \end{aligned} \quad (3.46)$$

with

$$C_i = \sqrt{V_{\Omega_i} \left(3 \cdot (6|B_{im}|)^2 + (3D \frac{|e_m|^2}{J_i^m})^2 \right)}. \quad (3.47)$$

3.2 The corner velocity interpolation with respect to mixed methods

In this section we will investigate the coercivity and inf-sup conditions when $W_h = W_h^{CVI}$, and Q_h is the space of constant pressures. Since we do not have $W_h \subseteq W$ on grids with curved faces, the inf-sup and coercivity conditions will not be considered for such grids.

Since $W_h^{CVI} = W_h^{RT_0}$ for parallelepiped grids, we know that both the inf-sup and coercivity conditions hold together with Q_h on such grids. The inf-sup condition does not hold together with pressure spaces of higher order. For the inf-sup condition, see [14], p. 235. The coercivity is easily

seen; if Ω_i is a parallelepiped, then both $\frac{dy_i}{dx}$ and $\frac{dw_i}{dx}$ are constants by (2.66) and (3.15), so the divergence has to be constant. If the fluxes add to zero, then

$$0 = \int_{\partial\Omega_i} w_i \cdot n \, dS = \int_{\Omega_i} \operatorname{div}(w_i) \, dy = V_{\Omega_i} \operatorname{div}(w_i), \quad (3.48)$$

so the divergence is necessarily zero, and thus we have $Z_h \subseteq Z$, which implies coercivity.

3.2.1 The coercivity condition

The previous example of the truncated pyramid can be used to prove that the CVI is not coercive on non-uniform grid refinements. We repeat the computations, for a scaled version of the cell, denoted Ω_h , with vertices

c_l	y
c_1	$(h, h, 0)$
c_2	$(2h, h, 0)$
c_3	$(2h, 2h, 0)$
c_4	$(h, 2h, 0)$
c_5	$(0, 0, h)$
c_6	$(3h, 0, h)$
c_7	$(3h, 3h, h)$
c_8	$(0, 3h, h)$

Until now we have used the subscript i to indicate the cell number. We now use the subscript h instead to indicate the cell size. First we have

$$w_h = -\psi_{h5} + \psi_{h6} = \quad (3.49)$$

$$\frac{1}{h^2} (1 - 8/9x_3)(t_{51}(1 - x_1)(1 - x_2) + t_{62}x_1(1 - x_2) + t_{73}x_1x_2 + t_{84}(1 - x_1)x_2) / \cos \theta. \quad (3.50)$$

Note that there is no subscript on θ since this angle is independent of h . The same holds for the tangents t_{lk} of the edges e_{lk} . If we compute the divergence of the CVI as in the above example we end up with

$$\operatorname{div}_y w_h = \operatorname{tr} \left(\frac{dw_h}{dx} \left(\frac{dy_h}{dx} \right)^{-1} \right) = \frac{1}{h^3} \frac{(28/9 + 8/9x_3 - 32/3x_3^2)}{(1 + 2x_3)^2}. \quad (3.51)$$

We then compute the W -norm,

$$\begin{aligned} \|w_h\|_W^2 &= \sum_k \|(w_h)_k\|_{L^2(\Omega_h)}^2 + \|\operatorname{div}(w_h)\|_{L^2(\Omega_h)}^2 = \quad (3.52) \\ \int_{\Omega_h} \sum_k (w_h)_k^2 + \operatorname{div}(w_h)^2 \, dy &= \int_K \left(\sum_k (w_h)_k^2 + \operatorname{div}(w_h)^2 \right) J \, dx \geq \int_K \operatorname{div}(w_h)^2 \, J \, dx = \\ \int_K \left(\frac{1}{h^3} \frac{(28/9 + 8/9x_3 - 32/3x_3^2)^2}{(1 + 2x_3)^2} \right)^2 h^3 (1 + 2x_3)^2 \, dx &= \\ \frac{1}{h^3} \int_K \frac{(28/9 + 8/9x_3 - 32/3x_3^2)^2}{(1 + 2x_3)^2} \, dx &= \frac{C_1}{h^3}. \end{aligned}$$

It is common to model the permeability as a constant function on each cell. When the grid is refined, the permeability should not vary, since it models a geological structure; ie. it is a feature of the domain Ω . See [1], p. 5. If we assume a coordinate system in which the permeability K is diagonal, then K^{-1} is also diagonal. We denote by r_k the elements of K^{-1} , and compute in a similar fashion

$$a(w, w) = \int_{\Omega_i} \sum_{k=1}^3 r_k (w_i)_k^2 dy = \int_K \sum_{k=1}^3 r_k (-\psi_{i5} + \psi_{i6})_k^2 J dx = \frac{C}{h}. \quad (3.53)$$

We can thus conclude that it is not possible to choose an grid-independent α such that the coercivity condition holds on this cell as $h \rightarrow 0$. Since it is not possible to find such an α for this cell, it is not possible to find such an α on any grid which insists keeping truncated-pyramid-like shapes as the grid is refined, and hence the CVI cannot be coercive on any such grid.

Note that the implication from this example rests on the shape of the cell, not whether the outer faces are curved or not, and this implies that the CVI is not coercive on such cells if we relax the assumption on the planarity of the outer faces either.

Two similar examples may be found in [1], pp. 121 and 126. The first example shows that $a(\cdot, \cdot)$ is not necessarily coercive outside Z_h , and the second is a case where $a(\cdot, \cdot)$ is not coercive on Z_h . In both these examples it is the large growth of the divergence which ruins the coercivity.

The large growth of the divergence can be expected to be the case for general hexahedra. We will now derive a general formula indicating how the divergence depends on h and the fluxes f_{ij} . Consider a general cell Ω_h with the vertices hc_l , $l = 1, 2, \dots, 8$. If we let $h \rightarrow 0$, then Ω_h , as in the previous example, does not change its shape as it contracts. We keep the notation with the subscripts h (here the subscript 1 means $h = 1$), and compute

$$\frac{dy_h}{dx} = h \frac{dy_1}{dx}, \quad (3.54)$$

which gives

$$\left(\frac{dy_h}{dx}\right)^{-1} = \frac{1}{h} \left(\frac{dy_1}{dx}\right)^{-1}. \quad (3.55)$$

Denote by A_{hj} the six areas of the faces of Ω_h . Since the shape of Ω_h is invariant with h , we may write

$$A_{hj} = h^2 A_{1j}. \quad (3.56)$$

This gives

$$w_h = \sum_{j=i}^6 f_j \psi_{hj} = \frac{1}{h^2} \sum_{j=i}^6 f_j \psi_{1j}, \quad (3.57)$$

and

$$\frac{dw_h}{dx} = \frac{1}{h^2} \sum_{j=i}^6 f_j \frac{\partial \psi_{1j}}{\partial x}, \quad (3.58)$$

where we have dropped one subscript from f_j , to stress that the fluxes can be chosen freely, and do not depend on h . If we now compute the divergence as in (3.33), then

$$\operatorname{div}_y(w_h) = \frac{1}{h^3} \left(\frac{dy_1}{dx}\right)^{-1} \left(\sum_{j=i}^6 f_j \frac{\partial \psi_{1j}}{\partial x}\right) = \frac{1}{h^3} C \cdot f, \quad (3.59)$$

where we have written $f = (f_1, \dots, f_6)$ and $C = (C_1, \dots, C_6)$ are the coefficients of the components of f . Clearly, C depends only the permeability K , and on the relative geometry of Ω_h , not its size. Recall that there are two conditions that imply $\operatorname{div}_y(w_h) = 0$; if Ω_1 is a parallelepiped or the fluxes f_j are uniform-flow-consistent. If neither of these is the case, the divergence can be expected to behave according to expression (3.59).

3.2.2 The inf-sup condition

We will now investigate the inf-sup condition for the CVI on a specific grid. For simplicity, Ω will be the unit cube, and the grid will be a $n \times n \times n$ distorted hexahedral Cartesian grid. A way to picture this is the cube Ω divided into n^3 distorted cubes Ω_i . 'Distortion' means here that every Ω_i is a perturbation, by a certain maximum percentage, of a cube of side $h = 1/n$. All Ω_i will have planar faces. A typical refinement of the grid doubles the number n , hence divides each Ω_i into eight new similar cubes, and the refined grid is accordingly a similar $2n \times 2n \times 2n$ Cartesian grid with $8n^3$ cells. It is easy to see that a $n \times n \times n$ Cartesian grid has a total of $3n^2(n+1)$ faces. See [9], chapter 5, for more details.

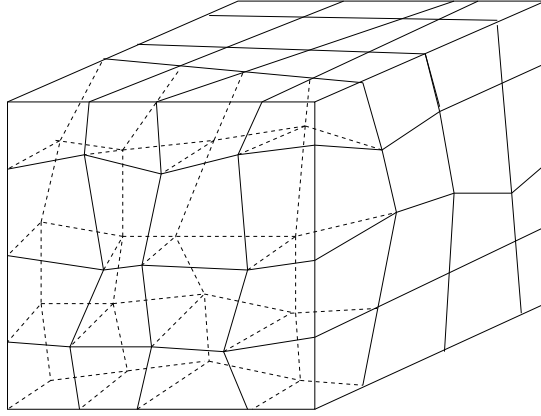


Figure 3.2: $4 \times 4 \times 4$ irregular Cartesian grid.

Recall from the preceding chapter that for the inf-sup condition, we have to check both if the spaces Q_h and W_h are balanced correctly against each other, else the condition might not be satisfied for any grid, and then whether $\lim_{h \rightarrow 0} \beta_h = \beta > 0$ as the grid refined. For non-parallelpiped grids with planar faces, the first is no problem in the combination CVI with constant pressure in each cell.

Theorem 3.2.1 *Together with the space of constant pressures in each cell, $Q_h = \{q; q|_{\Omega_i} = q_i \forall i\}$, there is a constant β_h such that CVI satisfies inequality (2.39) on each grid described above.*

Proof: In the described grid, the number of cells is n^3 , and the number of faces is $3n^2(n+1)$. Pick an arbitrary $q \in Q_h$, and a grid with cells Ω_i .

1. First of all, we obviously have

$$\|q\| \leq q_m \sqrt{V_\Omega} = q_m, \quad (3.60)$$

since Ω is the unit cube. Here $q_m = \max_i |q_i|$. Secondly, we can obtain a similar bound for the CVI,

$$\|w\| \leq Cn^3 f_m, \quad (3.61)$$

where $C = \max_i C_i$ (cf. eq. (3.46)), and $f_m = \max_i |f_{im}|$. With

$$\|q\| \|w\| \leq Cn^3 f_m q_m, \quad (3.62)$$

we have to show that given this q , it is possible to choose w (dependent on q) and β_h (independent of q) such that

$$\beta_h Cn^3 f_m q_m \leq b(q, w). \quad (3.63)$$

A natural question to ask now is how to maximize the form $b(q, w)$ given q and the maximal flux f_m . For our choice of Q_h , this is easy. We have (recall eq. (2.83))

$$b(q, w) = \sum_{i=1}^{n^3} q_i \sum_{j=1}^6 f_{ij}. \quad (3.64)$$

We rewrite this sum as

$$b(q, w) = \sum_j f_j (q_{j1} - q_{j2}) + \sum_k f_k q_k. \quad (3.65)$$

The first sum is over all interior faces of the grid, and the term $q_{j1} - q_{j2}$ is the pressure difference across the face j . The second sum is over all faces making up $\partial\Omega$, and q_k is the pressure of the boundary cell Ω_k . With formula (3.65) it is easy to see that to maximize $b(q, w)$ under the maximum norm, we have to set $f_j = f_m$ for all j ; each flux with the same sign as $q_{j1} - q_{j2}$ on each interior face (that is, from cells with high pressure towards cells of low pressure), and with the same sign as q_k on the boundary faces. Note that with this specification of the direction of the fluxes, all terms in (3.65) are positive.

2. We now construct the member of W_h for which (3.63) holds.

Case 1: If the maximum pressure q_m is in the cell Ω_k at $\partial\Omega$, then set the five interior fluxes of Ω_k to zero. We then have

$$q_m f_m \leq b(q, w) \quad (3.66)$$

since, as we can see from (3.65), every nonzero term of $b(q, w)$ is still positive after setting these five fluxes to zero.

Case 2: If q_m is in some interior cell Ω_i , then consider the following construction: build a sequence of adjacent cells until a cell Ω_k at $\partial\Omega$ is reached. For this 'corridor' of cells, we specify zero fluxes on the faces making up the boundary of this sequence with the rest of the grid, and compute

$$\sum_l b_l(q, w) = f_m (q_m + |q_k|) \leq b(q, w), \quad (3.67)$$

where the sum is over all cells in the sequence, and the last inequality holds for the same reason as in *Case 1*.

In any case, we now have

$$q_m f_m \leq b(q, w), \quad (3.68)$$

and if we set $\beta_h \leq 1/Cn^3$, then

$$\beta \|q\| \|w\| \leq q_m f_m \leq b(q, w), \quad (3.69)$$

which was the desired result. \square

This proves that the CVI, together with Q_h , defines a unique approximation on each grid. Unfortunately, we have reason to conjecture that existence of a β cannot be proved for our combination of Q_h and W_h on irregular grids with planar faces. We noted in the preceding section that on a truncated pyramid, the divergence of the CVI grows as f/h^3 as $h \rightarrow 0$. As explained in that section, this can be expected to be the case in general, and probably ruins the condition $\beta_h \geq \beta > 0$. To show this, we consider the inf-sup condition on a series of grids of the type described above. In the following, we will assume that the grid does not become uniform as it is refined, ie. that the cells are cubes always perturbed by a certain *minimum* percentage as $h \rightarrow 0$.

First set the pressure equal to the same constant, positive value q_0 in all cells. This gives

$$\|q\| = q_0 \sqrt{V_\Omega} = q_0, \quad (3.70)$$

since Ω is the unit cube. In the inf-sup condition, we divide by the pressure q_0 , which gives

$$\beta_h \|w\| \leq \frac{b(q_0, w)}{q_0} = \sum_{k=1}^{6n^2} f_k, \quad (3.71)$$

where we have used (3.65). The index k still ranges over the faces of $\partial\Omega$, and $6n^2$ is the number such faces. Since we want to find a w for each grid which minimizes $\|w\|$, we should clearly set all fluxes across interior edges to zero, as this does not influence $b(\cdot, \cdot)$, and any interior nonzero flux adds something to $\|w\|$.

We now take a closer look at $\|w\|$. We have

$$\sqrt{\int_{\Omega} \operatorname{div}(w)^2} \leq \|w\|, \quad (3.72)$$

and with all interior fluxes zero,

$$\int_{\Omega} \operatorname{div}(w)^2 dy = \sum_{i=1}^{m_1} \int_{\Omega_i} \operatorname{div}(w_i)^2 dy, \quad (3.73)$$

where i runs through the $m_1 \sim 6n^2$ boundary cells. Since the divergence on each cell can be expected to grow according to (3.59), we have

$$\int_{\Omega_k} \operatorname{div}(w)^2 dy = \frac{C_k f_k^2}{h^3}, \quad (3.74)$$

for all cells which have only one face at $\partial\Omega$, which gives

$$\frac{1}{h^3} \sum_{k=1}^m f_k^2 C_k \leq \int_{\Omega} \operatorname{div}(w)^2 dy, \quad (3.75)$$

where $m \sim 6n(n-2) \sim 6n^2$ is the number of such cells. Note that for some cells, for example the corner cells, which have three faces at $\partial\Omega$, expression (3.74) will be slightly different, since the divergence on such cells depend on three fluxes, not one. We can still write (3.75) as an inequality.

The question now is how the function

$$G(f) \stackrel{\text{def}}{=} \sqrt{\frac{1}{h^3} \sum_k f_k^2 C_k} \quad (\leq \|w\|) \quad (3.76)$$

behaves as the grid is refined. We have written $f = (f_1, f_2, \dots, f_m) \in \mathbb{R}^m$; the vector with the flux f_k as the k -th component. First note that as a function of the fluxes f_k , G is linear and passes through the origin on each straight line passing through the origin. This is seen by setting $f = dt$ for some $d = (d_1, d_2, \dots, d_m) \in \mathbb{R}^m$, which gives

$$\sqrt{\frac{1}{h^3} \sum_k (d_k t)^2 C_k} = t \sqrt{\frac{1}{h^3} \sum_k d_k^2 C_k} = Ct. \quad (3.77)$$

Since the constant C_k is only dependent on the geometry of Ω_k , not its size, as long as we do not alter the shape of the cells as the grid is refined, we can write

$$\sqrt{\frac{C_{\min}}{h^3} \sum_k d_k^2} \leq \sqrt{\frac{1}{h^3} \sum_k d_k^2 C_k}. \quad (3.78)$$

For the parametrization $f_k = d_k t$ we can choose

$$d_1^2 + d_2^2 + \dots + d_m^2 = 1 \quad (3.79)$$

as $n \rightarrow \infty$, which gives

$$\sqrt{\frac{C_{\min}}{h^3} \sum_k d_k^2} = \sqrt{\frac{C_{\min}}{h^3}} = \frac{C}{h^{3/2}}. \quad (3.80)$$

This is the slope of the function $G(f(t))$ with respect to t along the line $f = dt$. The slope of the function

$$H(f) \stackrel{\text{def}}{=} \sum_{k=1}^{6n^2} f_k \quad (3.81)$$

with respect to t along any line $f = dt$ is

$$\sum_{k=1}^{6n^2} d_k. \quad (3.82)$$

Under the constraint $d_1^2 + d_2^2 + \dots + d_{6n^2}^2 = 1$, this gradient clearly takes its maximum value along dt for

$$d_1 = d_2 = \dots = d_{6n^2} = \frac{1}{\sqrt{6n^2}}, \quad (3.83)$$

and the slope then equals $\sqrt{6n^2} \sim 1/\sqrt{h}$ with respect to t along this line. Since the direction of d was arbitrary and the slope of $G(f)$ along this direction grows with one order more as a function of h than the maximum slope of the function $H(f)$, we see that if the inf-sup condition is to hold on each grid, we have to let $\beta_h \rightarrow 0$ as $h \rightarrow 0$, and thus there is no $\beta > 0$ with $\beta \leq \beta_h$ as the grid is refined.

We observed in the preceding section that (3.59), and hence (3.80), equals zero if either the fluxes are uniform-flow-consistent or Ω_i is a parallelepiped. Uniform-flow-consistency is obviously not the case in this example since most cells have only one flux. It is also clear that if this example is to hold, then the grid has to be refined without letting the cells become parallelepipeds as $h \rightarrow 0$, as this would ruin the f/h^3 -growth of the divergence on which the example rests.

Chapter 4

Summary

We have seen that on parallelepipedic grids, the CVI is equal to the RT_0 space. This space is thoroughly described elsewhere.

On grids of non-parallelepiped cells with planar faces, the CVI is a member of $H(\text{div})$, but is not coercive together with any pressure space containing constants. It satisfies the inf-sup condition on each distorted cartesian grid with the space of constant pressures, hence will give a nonsingular linear system, and this result can obviously be extended to more general grids. The constant β_h is probably not bounded away from zero as the grid is refined. Of this we have sketched a proof, but more work would have to be done to make it rigorous.

For grids with non-planar faces the CVI does not reproduce fluxes correctly across curved faces except in special cases. This implies that it does not have continuity of the normal trace across cell boundaries, and thus the CVI is not a member of $H(\text{div})$ on grids with curved faces. Since the coercivity and inf-sup conditions do not hold with $\alpha > 0$ and $\beta > 0$ on general grids with planar faces, they cannot be expected to hold on general grids with curved faces either.

Proving convergence of the CVI together with constant pressures on non-parallelepiped grids with planar faces is probably nontrivial since the coercivity and inf-sup conditions are not satisfied. It was hoped that a mixed finite element method would benefit from the CVI's ability to reproduce uniform flow. We have not seen any indications on this as far as the inf-sup and coercivity conditions are concerned, but the question of whether this property affects the actual computations is still open.

Since the inf-sup and coercivity conditions are only sufficient conditions for convergence, not necessary, convergence might be possible to prove even though these conditions are not satisfied. However, this would probably be a very technical task, and thus numerical evidence of convergence should be collected before a non-standard attempt to prove convergence is made.

References

- [1] I.A. Aavatsmark. *Bevarelsesmetoder for elliptiske differensialligninger*.
- [2] R. A Adams. *Calculus*. Addison Wesley Longman, 2003.
- [3] K. Aziz and A. Settari. *Petroleum Reservoir Simulation*. Elsevier, 1983.
- [4] G.I. Barenblatt, V.M Entov, and V.M. Ryzhik. *Theory of Fluid Flow through Natural Rocks*. Kluwer, 1990.
- [5] J. Bear. *Dynamics of Fluids in Porous Media*. Dover, 1972.
- [6] S.C. Brenner and L.R. Scott. *The Mathematical Theory of Finite Element Methods*. Springer, 2002.
- [7] F. Brezzi and M. Fortin. *Mixed and Hybrid Finite Element Methods*. Springer, 1991.
- [8] L.C. Evans. *Partial Differential Equations*. American Mathematical Society, 1998.
- [9] H. Haegland, H.K Dahle, G.T. Eigestad, K.-A. Lie, and I.A. Aavatsmark. Improved streamlines and time-of-flight for streamline simulation on irregular grids. *Advances in Water Resources*, 30:1027–1045, 2007.
- [10] R.L. Naff, T.F. Russell, and J.D. Wilson. Shape functions for three-dimensional control-volume mixed finite element methods on irregular grids. *Developments in Water Science*, 42:359–366, 2002.
- [11] J.-C. Nedelec. A New Family of Mixed Finite Elements in 3D. *Numerische Mathematik*, 50:57–81, 1986.
- [12] J.M. Nordbotten and H. Haegland. On reproducing uniform flow on general hexahedra using one degree of freedom per surface. 2008.
- [13] Ø. Pettersen. Grunnkurs i reservoarmekanikk. 1990.
- [14] A. Quarteroni and A. Valli. *Numerical Approximation of Partial Differential Equations*. Springer, 1997.
- [15] O.V. Ushakova. Conditions of nondegeneracy of three-dimensional cells. a formula for a volume of cells. *SIAM Journal of Scientific Computing*, 23:1274–1290, 2001.
- [16] N. Young. *An introduction to Hilbert space*. Cambridge Mathematical Textbooks, 1988.